

# 1 When tree rings go global: challenges and opportunities for retro- 2 and prospective insight

3 Flurin Babst<sup>1,2,3\*</sup>, Paul Bodesheim<sup>4</sup>, Noah Charney<sup>5</sup>, Andrew D. Friend<sup>6</sup>, Martin P. Girardin<sup>7</sup>,  
4 Stefan Klesse<sup>3</sup>, David J.P. Moore<sup>8</sup>, Kristina Seftigen<sup>9</sup>, Jesper Björklund<sup>1,10</sup>, Olivier  
5 Bouriaud<sup>11</sup>, Andria Dawson<sup>8,12</sup>, R. Justin DeRose<sup>13</sup>, Michael C. Dietze<sup>14</sup>, Annemarie H.  
6 Eckes<sup>6</sup>, Brian Enquist<sup>5</sup>, David C. Frank<sup>1,3</sup>, Miguel D. Mahecha<sup>4</sup>, Benjamin Poulter<sup>15</sup>, Sydne  
7 Record<sup>16</sup>, Valerie Trouet<sup>3,8</sup>, Rachael H. Turton<sup>6</sup>, Zhen Zhang<sup>1,17</sup> & Margaret E.K. Evans<sup>3</sup>

8 <sup>1</sup>*Dendro Sciences Group, Swiss Federal Research Institute WSL, Zürcherstrasse 111, CH-*  
9 *8903 Birmensdorf, Switzerland*

10 <sup>2</sup>*W. Szafer Institute of Botany, Polish Academy of Sciences, ul. Lubicz 46, 31-512 Krakow,*  
11 *Poland*

12 <sup>3</sup>*Laboratory of Tree-Ring Research, University of Arizona, 1215 E Lowell St, Tucson, AZ-*  
13 *85721, USA*

14 <sup>4</sup>*Max Planck Institute for Biogeochemistry, Jena, Germany*

15 <sup>5</sup>*Department of Ecology and Evolutionary Biology, University of Arizona, Tucson AZ, USA*

16 <sup>6</sup>*Department of Geography, University of Cambridge, Cambridge, England*

17 <sup>7</sup>*Laurentian Forestry Centre, Natural Resources Canada, Quebec, Canada*

18 <sup>8</sup>*School of Natural Resources and the Environment, University of Arizona, Tucson, USA*

19 <sup>9</sup>*Department of Earth Sciences, University of Gothenburg, Gothenburg, Sweden*

20 <sup>10</sup>*Czech University of Life Sciences, Prague, Czech Republic*

21 <sup>11</sup>*Faculty of Forestry, Stefan cel Mare University of Suceava, Strada Universității 13,*  
22 *Suceava 720229, Romania.*

23 <sup>12</sup>*Department of General Education, Mount Royal University, Calgary, Alberta, Canada*

24 <sup>13</sup>*Rocky Mountain Research Station, US Department of Agriculture, Ogden UT, USA*

25 <sup>14</sup>*Earth and Environment, Boston University, USA*

26 <sup>15</sup>*NASA Goddard Space Flight Center, Greenbelt, Maryland 20771, USA*

27 <sup>16</sup>*Department of Biology, Bryn Mawr College, Bryn Mawr, USA*

28 <sup>17</sup>*Department of Geographical Sciences, University of Maryland, College Park, USA*

29 \*Corresponding author:

30 Dr. Flurin Babst

31 Swiss Federal Research Institute WSL

32 Zürcherstr. 111

33 8903 Birmensdorf

34 Switzerland

35 Email: [flurinbabst@gmail.com](mailto:flurinbabst@gmail.com)

36 Phone: +48 579 516 164

37 **Key words:**

38 Dendrochronology, scaling, data integration, climate change, forest growth, vegetation  
39 models, remote sensing, forest inventory, Anthropocene

40

41 **Abstract**

42 The demand for large-scale and long-term information on tree growth is increasing rapidly as  
43 environmental change research strives to quantify and forecast the impacts of continued  
44 warming on forest ecosystems. This demand, combined with the now quasi-global  
45 availability of tree-ring observations, has inspired researchers to compile large tree-ring  
46 networks to address continental or even global-scale research questions. However, these  
47 emergent spatial objectives contrast with paleo-oriented research ideas that have guided the  
48 development of many existing records. A series of challenges related to how, where, and  
49 when samples have been collected is complicating the transition of tree rings from a local to a  
50 global resource on the question of tree growth. Herein, we review possibilities to scale tree-  
51 ring data (A) from the sample to the whole tree, (B) from the tree to the site, and (C) from the  
52 site to larger spatial domains. Representative tree-ring sampling supported by creative  
53 statistical approaches is thereby key to robustly capture the heterogeneity of climate-growth  
54 responses across forested landscapes. We highlight the benefits of combining the temporal  
55 information embedded in tree rings with the spatial information offered by forest inventories  
56 and earth observations to quantify tree growth and its drivers. In addition, we show how the  
57 continued development of mechanistic tree-ring models can help address some of the non-  
58 linearities and feedbacks that complicate making inference from tree-ring data. By embracing  
59 scaling issues, the discipline of dendrochronology will greatly increase its contributions to  
60 assessing climate impacts on forests and support the development of adaptation strategies.

61 **1. Introduction**

62 *1.1. An increasing need to scale tree-ring data*

63 Climate change during the Anthropocene is now considered a certainty (Marotzke et al.,  
64 2017) and environmental research focuses increasingly on quantifying and forecasting the  
65 impacts of continued warming on ecosystems and natural resources. Forests receive  
66 particular attention because they absorb large amounts of excess atmospheric CO<sub>2</sub> generated  
67 by human activities (Le Quéré et al., 2016) and store this carbon in woody biomass for  
68 decades to centuries (Körner, 2017). Importantly, rising temperatures can have either  
69 beneficial or detrimental effects on forests, depending on their present climatic limitations  
70 (Babst et al., 2013; Charney et al., 2016; St George and Ault, 2014). For instance, climate  
71 warming in cold-humid areas can stimulate tree growth through a prolonged growing season  
72 and more rapid cellular development (Cuny et al., 2014; Rossi et al., 2016). In drier regions, a  
73 warming-induced increase in atmospheric water demand triggers physiological responses in  
74 trees that lower hydraulic conductivity, reduce the production and allocation of carbohydrates  
75 to structural growth, and ultimately increase tree mortality (Adams et al., 2017). This  
76 continuum of possible consequences from warming provides an incentive to understand how  
77 changes in the biotic and abiotic environment affect forest ecosystem processes across a  
78 range of spatial and temporal scales.

79

80 Measurements of secondary growth patterns in trees, shrubs, and perennial herbs  
81 (subsequently called “tree rings”) are the primary resource to retrospectively provide tree  
82 growth information across large environmental gradients and at sub-annual to multi-  
83 centennial time scales. Such data are increasingly used to study the impacts of global change  
84 on forest ecosystems. A number of recent studies have compiled large tree-ring networks to  
85 hind- and forecast forest growth variability in response to climate (Babst et al., 2013;

86 Charney et al., 2016; Martin - Benito and Pederson, 2015; Restaino et al., 2016; St George  
87 and Ault, 2014; Tei et al., 2017), track the recovery of growth after extreme events  
88 (Anderegg et al., 2015; Wu et al., 2017), relate growth variability to canopy dynamics  
89 (Vicente-Serrano et al., 2016, Seftigen et al., in press), or search for signals of CO<sub>2</sub>  
90 fertilization (Frank et al., 2015; Gedalof and Berg, 2010; Girardin et al., 2016; Peñuelas et al.,  
91 2011). In addition, tree-ring data are increasingly used to quantify aboveground biomass  
92 increment (Babst et al., 2014b), improve our physiological understanding of wood formation  
93 (Rathgeber et al., 2016), and calibrate mechanistic models for climate reconstruction (Guiot  
94 et al., 2014).

95

96 **Table 1:** Definitions of important terms used in this review (partly inspired by Scholes, 2017)

Term	Definition
Scale ( <i>noun</i> )	Spatial extent and/or temporal duration.
Scale ( <i>verb</i> )	Extrapolation or projection of a result from one scale to another. Herein, we focus primarily on the scaling of forest growth and biomass increment (as opposed to, e.g., scaling from local to global temperature variations; Neukom et al., 2014). Linear scaling (i.e., proportional or additive scaling) assumes that the driving processes are homogeneous over the scale range and that no interactions in space or time impose non-linearities. An example is the scaling of forest biomass increment from a sample of 0.1-hectare forest plots to a 10,000-hectare landscape. If heterogeneities (e.g., in forest type or time-since-disturbance) make simple linear scaling inaccurate, power-law scaling can capture nonlinearities across scales. For example, the scaling of bole diameter to whole-tree biomass involves allometric (power-law) equations, that are usually empirically derived, but may be (quasi-)mechanistic.
Downscaling	The process of disaggregation of a result to a smaller scale; i.e., a few-to-many problem. Climate system downscaling is a well-known example. The aggregated result is known; the challenge is to assign values (along with uncertainty) to the underlying subunits, according to some information about their heterogeneity.
Upscaling	The process of aggregation to a larger scale; i.e., a many-to-few problem. An example is the upscaling of information from many trees within a site to a single site-level estimate (e.g. a mean site chronology). Another example is the summing of biomass increment estimates from all trees in a forest plot to reach a stand-level estimate of biomass increment.

Resolution      Also known as “grain”, the smallest measurement unit in either space or time.

---

97

98 Tree-ring records are available on all forested continents (Babst et al., 2017; Brienen et al.,  
99 2016), inviting the use of existing and the development of new tree-ring archives for a variety  
100 of research contexts. However, tree rings remain a very local and variable product of tree-  
101 internal processes that are modulated by a tree’s immediate biotic and abiotic environment  
102 (Rathgeber et al., 2016). Inference and prediction at large spatial scales based on such local  
103 data (involving scaling, interpolation, and projection; Table 1) is challenging and introduces  
104 uncertainty that researchers need to be aware of and – to the extent possible – quantify  
105 (Figure 1). Scaling is complicated by heterogeneity (Scholes, 2017), for example when a tree-  
106 ring collection insufficiently represents forest structure, composition, and disturbance  
107 regimes across a landscape. Dendrochronologists often counteract heterogeneity by  
108 increasing the number of collected samples per tree, site, or region. This approach can indeed  
109 reduce uncertainties around the mean record for the desired scale (e.g. a site or regional  
110 chronology), but its success for improving spatial representation of tree growth critically  
111 depends on the underlying sampling strategy (see below). Another challenge for scaling is  
112 that fixed statistical relationships derived from a given dataset may not capture the high  
113 dimensionality in driver and response variables, their couplings, non-linear processes and  
114 feedbacks. This calls for a better understanding of the true variability in the system and  
115 ideally for mechanistic process representation to model tree growth (see Section 4). Given the  
116 above context, we find it prudent to briefly pause and examine the potential and challenges  
117 associated with scaling tree-ring information before making large-scale inference. Herein, we  
118 address the following three upscaling steps:

119

120 (A) **From the sample to the whole tree:** Tree-ring samples are collected as cross-sections,  
121 increment cores, or micro-cores. Regardless of the shape or size of samples, individual

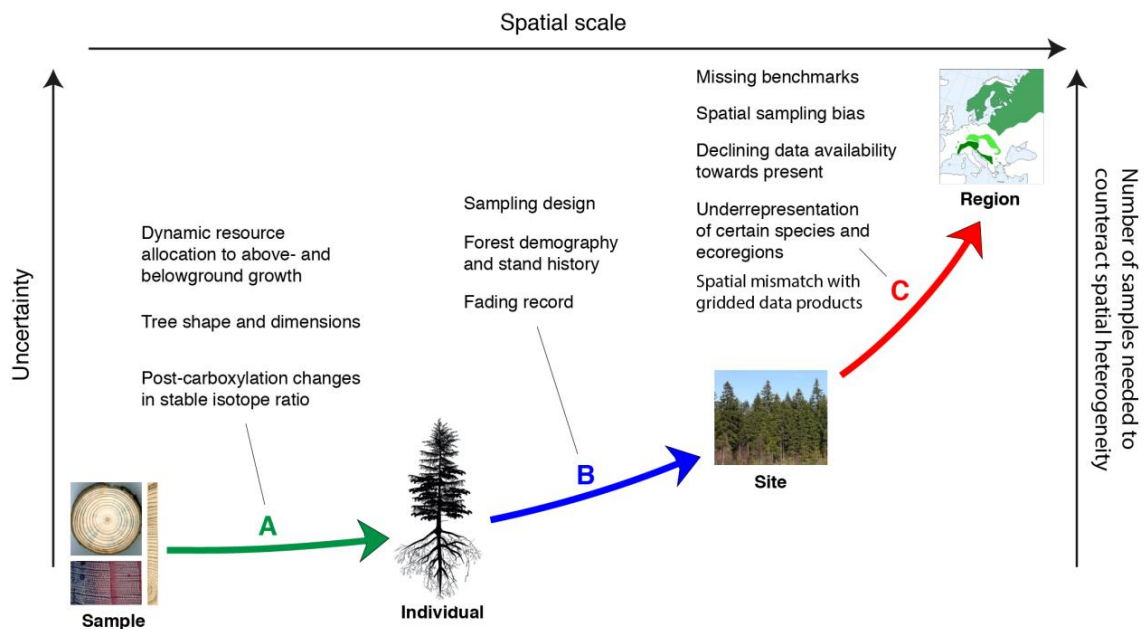
122 measurements capture growth only at one position along/around the stem, branch, or  
123 root. Multiple samples are thus often collected from the same individual to better capture  
124 its growth variability. After visually and statistically ensuring correct dating of each  
125 annual growth ring (i.e. “crossdating”; Black et al., 2016; Stokes and Smiley, 1968), the  
126 measurements of all samples are generally combined to represent the radial growth of  
127 the individual. This first step of upscaling (Table 1) usually involves averaging or  
128 pooling, but the representation of tree-level change may be with raw measurements,  
129 detrended and/or standardized tree-ring indices, conversion to basal area increment, or  
130 other forms of allometric scaling or structural modeling.

131 **(B) From the tree to the site:** A “site” is the area that encompasses the sampled individuals.  
132 Upscaling to the site level means combining the measurements from all individuals into  
133 one or multiple time series that are usually referred to as “chronologies”. An underlying  
134 assumption is thereby that the site is a subsample of a population of trees and the derived  
135 chronology is typically regarded as the best estimate of this population’s growth  
136 variability (Wigley et al., 1984). The criteria for sampling trees within a site vary  
137 according to the aims of a given study. For example, old and dominant individuals are  
138 selectively sampled for dendroclimatic reconstructions; plot designs, stratified or random  
139 samplings are often preferred for dendroecological studies; and trees with specific  
140 characteristics (e.g. scars) are targeted to assess the natural disturbance history of a site.  
141 Researchers are also interested in within-site variability that is driven by micro-site  
142 conditions (e.g. topography Salzer et al., 2014) and may contain relevant ecological  
143 information that is otherwise averaged out when only a mean site chronology is  
144 calculated (Buras et al., 2016; Peters et al., 1981).

145 **(C) From the site to larger spatial scales:** Site records are compiled into tree-ring networks  
146 to cover regions or continents. Depending on the research question, these networks are

147 either assessed in their entirety, or sites may be grouped and analyzed by species (Zhang  
 148 et al., 2018), growth variability (Seim et al., 2015), growth trends (Hellmann et al.,  
 149 2016), climate response (Babst et al., 2013; Björklund et al., 2017; Charney et al., 2016;  
 150 Martin - Benito and Pederson, 2015), or biogeography (Girardin et al., 2016). Moreover,  
 151 spatial assessments often include analyses of climate-growth relationships – sometimes  
 152 combined with clustering techniques, dimension reduction, or embedded in a machine  
 153 learning framework (see Section 2.2.1). The resulting regional records are assumed to  
 154 represent the geographic space covered by the underlying tree-ring network, an  
 155 assumption that will need thorough testing in the future (see Sections 2 and 5).

156



157

158 **Figure 1:** Overview of the different spatial scales and propagating uncertainty associated  
 159 with the scaling of tree-ring data. Sources of uncertainty are listed for each scaling step  
 160 (A-C) using Norway spruce (*Picea abies*) as an example. The sample images are adapted  
 161 from (Babst et al., 2014a) and the species distribution map is from  
 162 lutherie.net/eurospruce. If scaling steps A-C are carefully followed and uncertainties are  
 163 adequately considered, tree-ring data can theoretically meet the demand for global  
 164 information on long-term forest growth. In practice, however, a series of challenges  
 165 related to how, where, and when samples have been collected accompanies the transition  
 166 of tree rings from a local to a global data resource (see Section 1.2).

167 *1.2. Challenges associated with scaling tree-ring data*

168 Environmental systems are best represented if the collected data are extensive and distributed  
169 systematically or randomly across the target space (e.g. geographic or bioclimatic space).  
170 This is not the case for the vast majority of existing tree-ring records, in part because scaling  
171 was historically not the goal of dendrochronological sampling. Instead, data collection  
172 strategies and methods have been driven by study-specific goals, for example to date  
173 archaeological material, detect disturbance events, reconstruct climate, or assess the co-  
174 variation of tree growth with an environmental variable. Moreover, the scope of tree-ring  
175 research has continuously been expanded to include ecophysiology (Levesque et al., 2017),  
176 wood anatomy (von Arx et al., 2016), and growth phenology (Cuny et al., 2015; Trouet et al.,  
177 2012). This is fortunate because these emerging fields are considerably advancing our  
178 understanding of tree functioning, which will allow non-linearities and feedbacks to be  
179 mechanistically modeled and reconstructed (see Section 4). Yet, their sampling strategies are  
180 also not necessarily geared towards representing larger spatial scales with tree-ring  
181 observations. This diverse sampling background complicates upscaling of tree-ring  
182 information across all three steps:

183

184 **(A) Representing the whole tree:** Mature trees are usually sampled along the lower part of  
185 the stem, which is oldest and most accessible. How representative stem growth at this  
186 location is for the entire tree body depends on the dynamics of resource allocation and  
187 biomass formation. Assessing this variability would at a minimum require sampling  
188 individual trees at multiple heights, a laborious technique that is more readily applied to  
189 shrubs (Buchwal et al., 2013) but rarely performed on tall trees (but see e.g. Chhin et al.,  
190 2010; Monserud and Marshall, 2001; van der Maaten-Theunissen and Bouriaud, 2012).  
191 In addition, tree boles are never perfect cones and uncertainty due to collecting only few



192 samples around the stem needs to be reduced (Bakker, 2005). Another limitation of most  
193 existing tree-ring records is that tree dimensions (e.g. diameter and height) at the time of  
194 sampling have not been recorded. This hampers the estimation and reconstruction of  
195 whole-tree volume or biomass – and thus the representation of absolute growth (Babst et  
196 al., 2014b). Aside from physical sampling, our limited understanding of tree-internal  
197 processes can bias ecophysiological conclusions drawn from tree-ring data. For instance,  
198 tree-ring stable isotope ratios differ from those of freshly produced carbohydrates in  
199 leaves because additional isotopic fractionation and mixing occur during transport and  
200 transitory storage (Gessler et al., 2014). These effects are not well understood.

201 **(B) Representing the site:** A traditional focus of tree-ring sampling has been on old and  
202 dominant individuals of a single species (Cook et al., 1995) that respond to a strong  
203 common environmental driver. This approach has served to maximize the common  
204 growth variability among trees, which could then be used, e.g. as a proxy for  
205 instrumentally measured climate variables or to reconstruct disturbance events. Such  
206 selective sampling clearly hampers the objective of quantifying forest growth, because  
207 failure to represent the full tree population at a site and over time can severely bias tree-  
208 ring estimates of biomass accumulation (Brienen et al., 2017; Nehrbass - Ahles et al.,  
209 2014; Peters et al., 2015). In addition, the documentation of most tree-ring records in  
210 public archives (e.g. the International Tree Ring Data Bank; ITRDB) is insufficient in  
211 terms of site extent, species composition, and forest age or size structure.

212 **(C) Representing larger spatial scales:** To represent tree growth across regions or even  
213 continents, ideal networks of tree-ring sites densely cover the geographic extent of the  
214 study area and reflect, in proportion to the area they occupy, the range of bioclimatic and  
215 ecological conditions experienced by species within this area. This ideal has probably  
216 rarely been achieved. Instead, traditional sampling for dendroclimatological purposes has

217 often targeted areas with marginal growth conditions, which only occupy a small fraction  
218 of the landscape. We note, however, the difficulty of evaluating the spatial  
219 representativeness of existing networks because appropriate reference datasets are often  
220 lacking (see Section 2.1). If very large amounts of tree-ring data are compiled in mixed-  
221 species networks, their coverage can be more readily assessed. For example, a recent  
222 evaluation of the ITRDB indicated good coverage of climates with a mean annual  
223 temperature below 15 °C, whereas the spatial distribution of sites was strongly biased  
224 towards North America and Europe (Babst et al., 2017). Yet, even across these well-  
225 replicated continents, most records are subject to the above-mentioned sampling biases  
226 and the lack of biometric measurements restricts analyses to relative (i.e. detrended)  
227 growth variability and its climate response (Babst et al., 2013; Charney et al., 2016; St  
228 George and Ault, 2014). Going forward, it will be important to develop new tree-ring  
229 networks in more consistent and spatially representative ways (see Sections 2 and 3).

230

231 Uncertainties arising from the above-listed challenges may be more or less relevant in the  
232 context of a given study, but they generally propagate through all spatial scales (Figure 1).  
233 This does not preclude tree rings from being used in global research, but emphasizes the need  
234 to i) understand how data are derived and ii) carefully treat data with explicit characterization  
235 of uncertainties. Hereafter, we review possibilities to facilitate the scaling of existing and  
236 newly collected tree-ring data with emphasis on quantifying tree growth and its drivers across  
237 increasingly large geographic and bioclimatic domains. In Section 2, we discuss statistical  
238 approaches to derive spatial patterns from existing networks, such as the ITRDB. Section 3  
239 highlights possibilities to produce spatially explicit records of forest growth, by integrating  
240 the temporal information from tree rings with the spatial information from forest inventories  
241 and remotely sensed earth observations. Section 4 describes tree-ring and vegetation models

242 of increasing complexity and scope that can provide a mechanistic understanding of tree  
243 growth, which is particularly relevant for predictions into future time frames. In addition to  
244 this general review, we provide in each section a practical and illustrative example related to  
245 tree ring-based inference at large scales. We end our article with some perspectives for future  
246 research.

247

## 248 **2. Spatial patterns from detrended tree-ring data**

### 249 *2.1. On the climate sensitivity bias in global archives*

250 Assessing the relationships between tree growth and monthly to seasonal climate has been a  
251 core objective of many tree-ring network analyses. This is because climate is the most  
252 important driver of inter-annual growth variability around the globe (St George and Ault,  
253 2014) and long-term instrumental records of temperature, precipitation, and derivatives  
254 thereof are readily available. The obtained statistical relationships between radial tree growth  
255 and climate variation are strongest in areas where one or few climate parameters are highly  
256 limiting for growth (Fritts, 1976), for example at the cold or dry edge of a species'  
257 distribution range. These marginal growth environments (where trees often also live long) are  
258 frequently targeted by dendroclimatologists to maximize the co-variation of the tree-ring  
259 proxy with the desired climate parameter for reconstruction (e.g. Wilson et al., 2016). Hence,  
260 it seems likely that – even though palaeoclimatology is only one facet of tree-ring research –  
261 marginal sites are overrepresented in global tree-ring archives. Depending on its severity, this  
262 bias may enhance the derived magnitudes and biogeographic patterns in the climate response  
263 of forests (Babst et al., 2013; Charney et al., 2016; St George and Ault, 2014; Zhang et al.,  
264 2018) and the networks cannot be considered to be fully representative of forest growth at  
265 large scales.

266

267 Quantifying this potential oversensitivity to climate in large tree-ring archives requires the  
268 development of new, representative reference networks (see Section 3.1). Initial research in  
269 this direction suggests considerable geographic variation in the magnitude of the climate  
270 sensitivity bias. For example, Klesse et al (in review a) found that ITRDB tree ring-width  
271 records in the US Southwest were 40 to 60% more sensitive to climate variation than  
272 surrounding samples collected in forest inventory plots. When the two datasets were used to  
273 estimate growth trends in response to projected climate change through 2099 in this region,  
274 the ITRDB trees implied a 41% greater decline in growth compared to the representative  
275 forest inventory sample. By contrast, a Europe-wide comparison of tree-ring data from the  
276 ITRDB against a newly collected network of sample plots showed no significant difference in  
277 climate sensitivity (Klesse et al. in review b). Hence, a general statement on the magnitude of  
278 the climate sensitivity bias in the ITRDB cannot be made at this point. Further evaluation  
279 efforts – including collating existing data not available through public repositories and/or  
280 developing new networks of tree-ring records – will be crucial to quantifying existing biases  
281 and increasing the representativeness of tree-ring archives for global forest growth. Also,  
282 further work on defining and using consistent metrics for sensitivity may be required to  
283 elucidate the magnitude and characteristics of this bias.

284

## 285 *2.2. Statistical projection of relative growth variability*

286 The collection of dense tree-ring networks worldwide and in near real-time is impractical.  
287 Hence, the goal of upscaling from sites to landscapes (scaling step C, Figure 1) has to be  
288 achieved via the statistical projection (or mechanistic modeling, see Section 4) of tree growth  
289 across areas where measurements are missing. This is possible using empirically calibrated  
290 relationships between tree growth and its abiotic drivers. One limitation of this approach,  
291 however, is the small number of available predictor variables that are spatially resolved and

292 cover sufficiently long time scales. Indeed, most remotely sensed earth observation records  
293 (e.g. of soil moisture, land cover, or forest disturbance regimes) are still not long enough to  
294 allow for the calibration of robust statistical models that could be used to predict tree growth.  
295 This leaves long-term gridded climate products (e.g. Harris et al., 2014) as the only option,  
296 with associated caveats when used in the context of bioclimatic niches (Ols et al., 2017).  
297 Predicting growth variability from climate alone is clearly a simplification of the highly  
298 complex set of drivers and responses that shape forests. Accordingly, higher-end calibration  
299 statistics for temperature reconstruction have achieved around 50-60% of the variance  
300 explained for the instrumental target (Wilson et al., 2016), whereas seasonal climate-growth  
301 relationships that emerge from large networks are on average much weaker (St George and  
302 Ault, 2014). In addition, the seasonality in climate response changes considerably between  
303 species and across climate space (Babst et al., 2013; Cook et al., 2001; Teets et al., 2018),  
304 making it impossible to globally attribute growth variability to climate during a single season.  
305 For all these reasons, novel and creative statistical approaches are needed to project radial  
306 growth variability at large spatial scales.

307

### 308 *2.2.1 Practical Example 1: Towards gridded tree-ring width anomalies for Europe*

309 Here we present and evaluate a machine learning approach to produce gridded tree-ring  
310 products at continental scales. We thereby pursue a purely statistical approach (as opposed to  
311 mechanistic formulations of biophysical processes; see Section 4) and estimate relative radial  
312 growth variability from a set of climatic predictor variables in a regression model. We used  
313 random decision forests (RDF; Breiman, 2001), a well-established technique that provides a  
314 flexible framework for learning nonparametric and nonlinear relationships when faced with  
315 many and collinear predictors. Our RDF models each contained 100 random decision trees  
316 and the final tree-ring width anomalies were predicted by averaging the outputs of each

317 individual decision tree to prevent overfitting. RDF models need to be trained with observed  
318 datasets (Figure 2). For this we used European tree-ring width chronologies from the ITRDB,  
319 detrended with a 30-year cubic smoothing spline, and climate data from the corresponding  
320 CRU TS-3.22 grid cells (Harris et al., 2014). Climate variables included monthly minimum,  
321 mean and maximum temperature, diurnal temperature range, ground frost frequency,  
322 precipitation, wet day frequency, vapor pressure, potential evapotranspiration, and cloud  
323 cover. Climate data from the preceding and current years (24 months in total) were entered in  
324 the model to account for lag effects frequently observed in tree-ring data (Zhang et al., 2018).  
325 The ITRDB contains enough data (~1000 European sites) to train individual RDF models  
326 separately for the most frequent tree genera (Table 2), many of which are primarily  
327 represented by one species. In addition, we trained a model where sites from all genera were  
328 pooled together. To evaluate model performance, we applied a leave-one-site-out cross-  
329 validation, under the condition that a specific chronology was only estimated based on other  
330 sites of the same genus that do not fall within the same CRU TS-3.22 grid cell (i.e. to prevent  
331 biases).

332

Genus	Monthly predictor variables		Seasonal predictor variables	
	MEF	RMSE	MEF	RMSE
<i>Abies</i>	0.329	0.146	0.261	0.527
<i>Fagus</i>	0.313	0.179	0.257	0.512
<i>Larix</i>	0.158	0.204	0.090	0.302
<i>Picea</i>	0.310	0.127	0.245	0.515
<i>Pinus</i>	0.240	0.130	0.173	0.430
<i>Quercus</i>	0.326	0.136	0.267	0.534
All sites	0.287	0.145	0.225	0.485

333 **Table 2:** Performance of random forest regression models for predicting the growth  
334 variability of individual tree genera across Europe, assessed with a leave-one-site-out  
335 validation. Seasonal climatic predictors were aggregated for both the previous and current  
336 years (March – May; June – August; September – November) and the winter in between  
337 (December – February). MEF – Nash-Sutcliffe modeling efficiency; RMSE – root mean  
338 square error

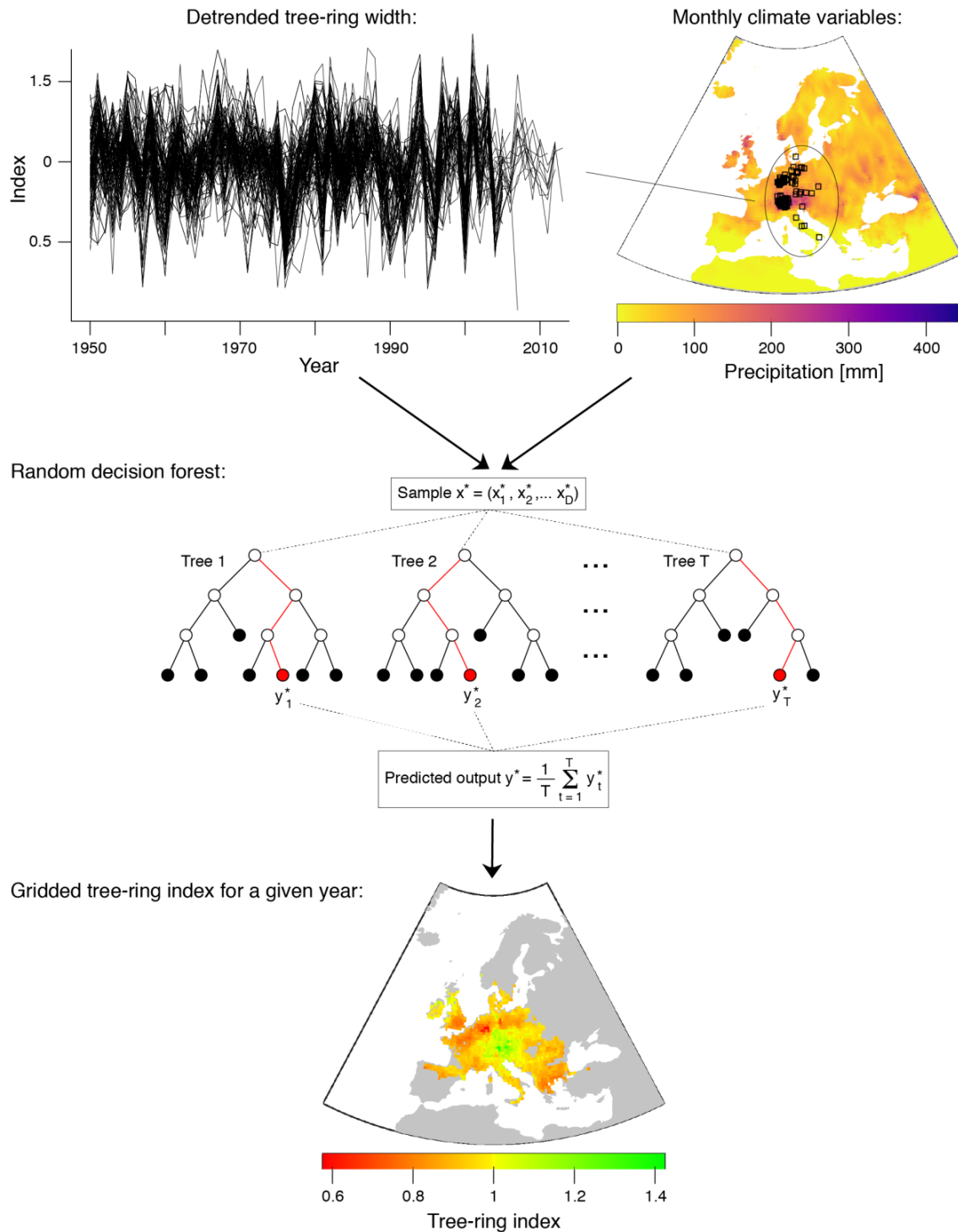
339  
340 Across the entire European network, approximately 29% of the variance was explained (i.e. a  
341 Nash-Sutcliffe modeling efficiency (MEF; Nash and Sutcliffe, 1970) of about 0.29; Table 2).  
342 Importantly, RDF models with monthly predictors yielded stronger predictive accuracy  
343 compared to those with seasonally aggregated predictors. This emphasizes the relevance of  
344 changing seasonality in climate response across the represented climatic domains (Babst et al.,  
345 2013). The RDF models for individual genera performed similarly to the overall model (31-  
346 33% explained variance), except for *Larix* and *Pinus* where MEF was lower. For *Larix*, this  
347 is likely due to well-documented periodic defoliation by the Larch budmoth (Esper et al.,  
348 2007), which negatively affects growth and partly decouples it from its climatic drivers.  
349 Excluding known budmoth years is thus a possibility to improve future RDF predictions. For  
350 *Pinus*, the lower RDF performance could simply be related to the large number of *Pinus*  
351 species that are represented on the ITRDB, which increases both the distribution range and  
352 the diversity in climate response.

353

354 After the training phase described above, the inferred RDF models were combined with the  
355 gridded data products of the CRU TS-3.22 dataset to project radial growth anomalies across  
356 Europe, yielding annual raster maps of relative growth variability for each tree genus (Figure  
357 S1, Appendix A). Projection excluded those areas falling outside the geographic distribution  
358 of a given genus (referencing the 1 km<sup>2</sup> resolution distribution maps in the European Atlas of  
359 Forest Tree Species; de Rigo et al., 2016). Accordingly, a CRU TS-3.22 grid cell (0.5°  
360 resolution) was included, if it covered at least one smaller grid cell from the distribution maps  
361 that reported a presence of the genus at >5%. Encouragingly, our first results show clear  
362 differences in spatial growth variability among genera (Appendix A), even for those that  
363 belong to the same plant functional type. In addition to attributing these patterns to specific  
364 drivers, we are working on improving the RDF performance. This can potentially be achieved

365 by including not only the inter-annual climate variability in the models, but also the long-  
366 term mean climatic conditions at each site. This way, the contrasting effects of, for instance, a  
367 warm anomaly under cold-humid (expected growth increase) vs. hot-dry (expected growth  
368 decrease) conditions can be better accounted for. Investigations at the species-level, rather  
369 than the genus-level, could also be explored in the future for potential improvements in  
370 modeling skill. In addition, we aim to consider non-climatic drivers in the RDF models as  
371 suitable spatial data become available.





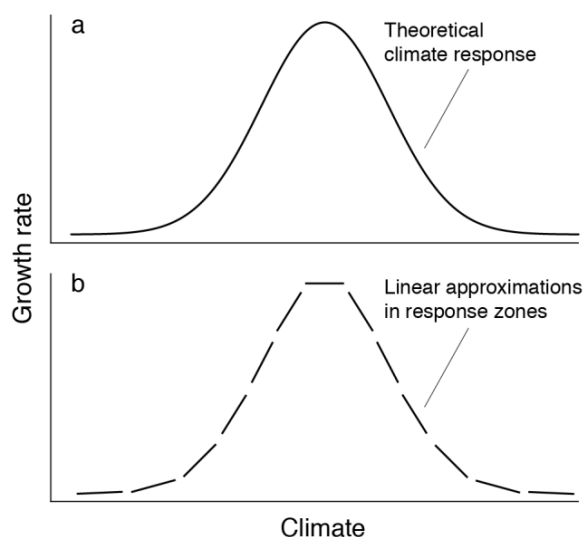
372

373 **Figure 2:** Random decision forest approach to produce gridded projections of radial tree  
 374 growth variability. This example includes all *Fagus sylvatica* sites that were available from  
 375 the International Tree-Ring Data Bank as of October 2016.

### 2.3. Spatially varying climate responses of radial tree growth

The statistical exercise presented in Section 2.2.1 assumes that the derived climate-growth relationships apply throughout the study domain, either across all species or in taxonomic groups (genera) – an assumption that we address in the following. It also showed that predicting relative growth variability from climate variability alone leaves a considerable fraction of the variance unexplained. By contrast, changes in the underlying climate-growth relationships should be more straightforward to predict and project because they follow gross biogeographic patterns (Babst et al., 2013; Charney et al., 2016). Indeed, a substantial body of literature has successfully mapped historical climate-growth relationships across space and time (Martin - Benito and Pederson, 2015; Restaino et al., 2016; St George and Ault, 2014). However, if the goal is to interpolate local observations of climate response across the intervening geographic space between unevenly distributed sites, a series of spatial challenges emerges. A first challenge relates to differences in the climate response among species at a given location (Teets et al., 2018). Accounting for such differences requires high-resolution maps of species composition for the entire target region, which may not exist everywhere and/or lack *in-situ* quality assessment (Serra-Diaz et al., 2017). Hence, the influence of species composition on the climate response of forests remains difficult to assess at large scales (Grossiord et al., 2014). A second challenge stems from limited information on micro-climate, nutrient availability, hydrology and topography. Such abiotic micro-site conditions can alter the climate response of trees (Nicklen et al., 2016; Salzer et al., 2009), but high-resolution data across the scaling area are rarely available. These two challenges are compounded by a third challenge: a shortage of tree-ring data for many species and certain ecoregions, especially in the tropics, that are severely under-represented in public archives (Babst et al., 2017).

401 These spatial challenges require finding a balance between the level of detail that is  
402 considered in an analysis, and the spatial scale that can be reached with the available data.  
403 One relatively simple option is to construct a single statistical model that describes growth as  
404 a function of the climatic niche that encompasses all trees within the scaling region,  
405 regardless of species (e.g. the “all sites” RDF model in Section 2.2.1). If we looked at a slice  
406 of this growth-climate function along one climate axis of the niche, we would expect it to  
407 look unimodal (Figure 3a). However, the underlying function is multivariate, nonlinear, and  
408 relatively data-intensive to parameterize. In addition, this approach ignores species-specific  
409 drivers of tree growth (including pests and pathogens, Esper et al., 2007) and assumes that  
410 spatial differences in climate response can be solely attributed to gradients in the baseline  
411 climate, rather than to differences in species composition, competition, or other co-variables.  
412 In other words, site- and species-specific characteristics are averaged out for the sake of  
413 generalization, which may be necessary to reach very large spatial domains. In a global  
414 context, it may be plausible to subject all species to the same treatment because  
415 biogeographic patterns in climate response are generally more pronounced than differences  
416 between species (Fritts 1976).



417  
418 **Figure 3:** Idealized growth rate as a function of a single climate variable across the target  
419 niche (a). This function can be approximated by a series of linear segments obtained from

420 local climate response zones (b).

421

422 A refined version of this approach, while still pooling all species, is to construct separate  
423 growth-climate functions for geographic sub-areas (“response zones”) of the target domain  
424 (Charney et al., 2016). This allows approximating the global response curve with a series of  
425 local linear models specific to these response zones (Figure 3b). The zones themselves could  
426 be based on existing ecoregions (Omernik and Griffith, 2014) or other (e.g. geological)  
427 criteria to account for some of the missing non-climatic co-variates. Alternatively, they can  
428 be inferred from the climate responses contained in the tree-ring time series themselves. For  
429 instance, Charney et al. (2016) defined response zones by first clustering tree-ring sites across  
430 North America based on their climate correlation functions and then used an RDF analysis to  
431 assign all grid cells on the landscape to one of the clusters according to their baseline  
432 climates. This has the significant advantage that, as baseline climates shift in the future, both  
433 geographic (i.e. poleward) shifts in the response zones and changes in the climate sensitivity  
434 itself can be accounted for. Moving forward, a further refinement could be to capture  
435 variation in the local slopes of climate-growth relationships using models that include both  
436 long-term baseline climates and short-term climate anomalies (and interactions between  
437 them) as predictors of growth. In particular, this would capture continuous variation in  
438 climate-growth responses across climatic gradients.

439

440 Clearly the most precise approach would be to construct the growth-climate function  
441 including the effects of individual species. Besides considering species-specific  
442 characteristics, this would also account for the fact that populations near the distribution limit  
443 are genetically adapted to respond less strongly to variability in limiting climatic drivers  
444 (Housset et al., 2018). However, detailed maps of species locations and composition would  
445 still be required to represent the actual climate response at a given location (de Rigo et al.,

446 2016; Serra-Diaz et al., 2017) and weight the species-specific responses in a mixed species  
447 system. In addition, representative tree-ring data from across the entire target space are  
448 needed, which are currently not available for most species. Establishing this observational  
449 basis through data mining initiatives and especially the development of new and spatially  
450 representative tree-ring networks will be key to enabling the projection of species-specific  
451 climate responses with precision.

452

453 In contrast to the spatial challenges described above, temporal limitations to empirically  
454 forecasting the climate response will not be resolved by extensive and representative  
455 sampling. One reason for this is that the overlap between tree-ring and instrumental data is  
456 often limited to a few decades and extrapolation to future time frames is thus based on  
457 relatively short-term observations. This is problematic because the climate response is not  
458 only determined by how tree growth responds to climate on an inter-annual basis, but can be  
459 modified by longer-term climate patterns (Madrigal-González et al., 2017; Mendivelso et al.,  
460 2014) that are not captured in short time series. In addition, there may be a compounding  
461 effect when “ecological memory” leads to lagged responses after disturbances or climate  
462 anomalies (Ogle et al., 2015), or when a recurring climate anomaly alters the growth response  
463 itself (Brzostek et al., 2014; Galiano et al., 2012). For example, one hot summer may lead to  
464 only a minor decrease in growth rate in a drought-prone region, whereas a sequence of hot  
465 summers can cause increasingly dramatic growth declines. By contrast, there can be  
466 acclimation, wherein the recurrence of a climate anomaly (e.g. drought) lessens the strength  
467 of the growth response (Ainsworth and Long, 2005; Farris et al., 2015). This is possible  
468 because trees are plastic organisms that can shift their resources over time, e.g. by growing  
469 more roots, restructuring branches, thickening the bark, or decreasing leaf size. Such  
470 physiological changes allow trees to better conserve water and return to normal growth more

471 rapidly after a drought episode. Moreover, ecosystem-level responses to climate change will  
472 also influence the growth of trees. For example, drought induced mortality (Adams et al.,  
473 2017) often results in a reduction in stand density and living biomass. This process is similar  
474 to selective thinning that enhances growth and survival by sharing of available resources  
475 amongst fewer individuals (Clark et al., 2016). In addition, when we aim to forecast over  
476 time periods of generations, we have to consider the possibility of genetic adaptation and  
477 species migration (Aitken et al., 2008; Housset et al., 2018). Both of these processes tend to  
478 make future generations of trees growing at a location better suited to the new climate than  
479 the preceding generations. Finally, the trees of the future are likely to experience different  
480 combinations of temperature, precipitation, and atmospheric CO<sub>2</sub> concentrations than those in  
481 the past (Ainsworth and Long, 2005; Frank et al., 2015). Hence, any attempt to statistically  
482 forecast based on stationary observations from the past is always associated with increased  
483 uncertainty (Gustafson, 2013). For all of these reasons, an advanced mechanistic  
484 understanding of tree growth and climate response is needed (see Section 4).

485

### 486 **3. Integration of tree rings with other ecological or Earth observations**

487 Tree-ring data offer decadal- to multi-centennial-length records of radial tree growth at  
488 annual to sub-annual resolution, allowing growth variability and its drivers to be investigated  
489 through time. However, quantifying absolute tree- and site-level growth (scaling steps A and  
490 B, Figure 1) from tree rings requires additional information about tree architecture (i.e.  
491 allometries) and forest stand characteristics. This information is increasingly available from  
492 forest inventories and remotely sensed earth observations. In turn, tree-ring data can help  
493 compensate for the coarse temporal resolution of forest inventories (plots are typically  
494 revisited once every 3-10 years) and the generally short time-series of both data streams.  
495 Bringing together the temporal and spatial strengths of these three types of observations

496 provides new opportunities to quantify tree growth across a range of scales (Zuidema and  
497 Frank, 2015).

498

### 499 *3.1. Forest inventories*

500 Tree rings have been used to assess tree growth in a forestry context since the mid-19<sup>th</sup>  
501 century, but it is only recently that collections made by forest inventory programs or in other  
502 permanent sample plots are being developed into data networks. Examples of these initiatives  
503 include Canada (Duchesne et al., 2017), the western United States (DeRose et al., 2017),  
504 Romania (Bouriaud et al., 2016), Mexico (G. Gutierrez-Garcia, pers. comm.), and parts of the  
505 tropics (Brienen et al., 2016). These data have been used, for instance, to detect signals of  
506 CO<sub>2</sub> fertilization (Girardin et al., 2016) or to assess shifts in growth response to climate  
507 (Charru et al., 2017; D'Orangeville et al., 2016). Here we describe opportunities to quantify  
508 trends and temporal variability of tree growth that emerge from this type of tree-ring network.  
509 We also discuss statistical tools for integrating tree-ring with forest inventory data and  
510 thereby move beyond the traditional statistical modeling based solely on the principle  
511 limiting factors (Fritts, 1976). Finally, we identify some of the challenges that remain for  
512 combining tree-ring and forest inventory data into long-term records.

513

514 Collecting tree-ring data in a forest plot context can have three major advantages with respect  
515 to the scaling and projection of growth or aboveground biomass increment (ABI): 1)  
516 sampling can be performed in a comparatively representative or unbiased manner, 2) absolute  
517 rather than relative tree growth can be quantified, and 3) the inventory offers complementary  
518 information on the characteristics of the forest stand in which a tree is growing. Together,  
519 these advantages help overcome some of the limitations for estimating biomass growth  
520 associated with traditional tree-ring sampling (see Section 1.2). National forest inventory

521 (NFI) programs are specifically designed to make estimates of forest characteristics (area or  
522 volume of forest; number and dimensions of trees) at large spatial scales from carefully  
523 designed networks of sampling plots (Bechtold and Patterson, 2005). The design may vary  
524 from one political entity to another (McRoberts et al., 2009), but their spatial representation  
525 of forested areas is essentially unparalleled. Within plots, the collection of increment cores in  
526 an objective manner with respect to tree species and size or age classes attempts to make  
527 sampling more representative of a forest (and overall forest growth) compared to that  
528 designed for dendroclimatological purposes (Nehrbass - Ahles et al., 2014). Tree-ring data  
529 collected in forest plots that are not part of an NFI (e.g. (Davis et al., 2009; Klesse et al.,  
530 2016) also make useful contributions to the overarching goal of building representative  
531 networks, particularly when the plots are arranged along environmental gradients (e.g.,  
532 Buechling et al., 2017; Foster et al., 2016; Rollinson et al., 2016; Sánchez-Salguero et al.,  
533 2015). Ensuring “representativeness” within forest stands and across landscapes is key to  
534 addressing the heterogeneities, nonlinearities, and feedbacks that make scaling a challenge  
535 (Scholes, 2017).

536

537 Increment cores collected in forest plots are usually associated with measurements of tree  
538 dimensions and stand conditions. A measurement of diameter at breast height (DBH) at the  
539 time of sampling makes it possible to reconstruct annual tree diameter (Bakker, 2005), which  
540 can then be transformed into absolute estimates of tree growth (Alexander et al., 2017; Babst  
541 et al., 2014b). Analyzing absolute growth is key to addressing questions about the role of  
542 forests in the terrestrial carbon cycle and integrating tree-ring data with observed or simulated  
543 forest productivity (Babst et al., 2014a, Klesse et al. in review b). In this context, metrics like  
544 basal area increment (BAI) and ABI are more useful and interpretable than relative growth  
545 variability generated by detrending raw tree-level measurements (Cook et al., 1995) to

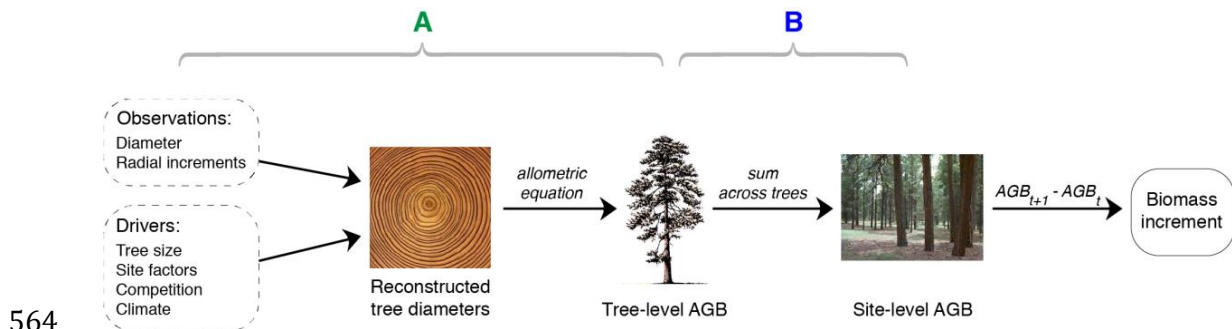


546 construct a site-level chronology. Besides the associated loss of inter-tree variability in  
 547 absolute growth rates, detrending is one of the most subjective and debated aspects of tree-  
 548 ring research because the choice of method critically affects the environmental information  
 549 that is preserved in ring-width time-series (Cook, 1987; Melvin and Briffa, 2008; Sullivan  
 550 and Csank, 2016).

551

552 Individual tree growth is also influenced by competition from neighboring trees, and in a  
 553 carbon accounting context it becomes critical to quantify, understand, and project such  
 554 demography-driven changes in forest growth (Chen et al., 2016; Trotsiuk et al., 2016).  
 555 Capturing the influence of competition on individual tree growth is also key to scaling step B  
 556 (Figure 4) because individual tree growth both influences and is influenced by forest stand  
 557 basal area, forming a self-regulating (density-dependent) feedback. Tree-ring data collected  
 558 in a forest plot context allow for modeling the influence of forest stand conditions explicitly,  
 559 as exemplified in several recent studies (Buechling et al., 2017; Foster et al., 2016; Rollinson  
 560 et al., 2016; Sánchez-Salguero et al., 2015). Accounting for such *in-situ* information in  
 561 statistical models is expected to produce more realistic predictions of tree growth compared  
 562 to those based exclusively on climate variability.

563



564

565 **Figure 4:** Scaling of tree growth from observations of bole diameter and tree-ring width to  
 566 tree- and site-level aboveground biomass (AGB) involves upscaling steps A and B. Forest

567 plot data provide information on the drivers of tree growth, including site factors such as  
568 slope, aspect, soil conditions, stand-level basal area, and climate.

569  
570 These three characteristics of tree-ring data collected in a forest plot context –  
571 representativeness, absolute growth, and accompanying information on the forest stand and  
572 sampling design therein – enable the scaling from individual observations of bole diameter  
573 and radial increments to stand- and landscape-scale biomass accumulation (Figure 4). Annual  
574 reconstructions of DBH can be transformed to whole tree biomass increments using  
575 allometric equations (scaling step A; Forrester et al., 2017). We note that the use of  
576 allometric equations is associated with its own set of uncertainties (Alexander et al., 2017;  
577 Nickless et al., 2011), some of which can be constrained with additional information derived  
578 from tree rings. For example, time series of wood density variation, combined with allometric  
579 estimates of tree volume, can improve estimates of whole-tree biomass increment (Bouriaud  
580 et al., 2015; Clough et al., 2017). Tree-level biomass increment can then be summed across  
581 individuals in the plot and adjusted by a known expansion factor (step B). Subsequently, the  
582 plot-level biomass estimates can be scaled to the target population using plot-level expansion  
583 factors or pre-determined sample-based estimators (Bechtold and Patterson, 2005).  
584 Alternatively, plot-level estimates are projected onto some other spatial scale using remote  
585 sensing observations (step C; Section 3.2; Jucker et al., 2017).

586

587 Integration of tree-ring and other forest inventory data can also take the form of data  
588 assimilation. The two data streams can, for example, be assimilated using a state-space model  
589 (Clark et al., 2007), or a hierarchical Bayesian model with two respective regressions linked  
590 by a constant of proportionality (Evans et al., 2017). Both of these statistical approaches can  
591 additionally take advantage of bole diameter re-measurement data for mixed datasets  
592 composed of trees with and without increment cores, and model the multiple influences on  
593 the growth of all individual trees explicitly. Assimilation of these two sources of information

594 that describe the common process of tree growth advances our understanding of that process,  
595 while refining estimates of both process variability and measurement uncertainty. The ability  
596 to quantify both process variability and measurement uncertainty provides the opportunity to  
597 improve reconstructions and forecasts of forest growth and productivity at sites for which  
598 only one data type is available (Dietze, 2017). Finally, if forest inventory records are  
599 sufficiently long to inform about forest mortality, it becomes possible to characterize the  
600 relationship between growth and mortality. With a better understanding of the growth-  
601 mortality relationship, forest growth and productivity can be reconstructed further back in  
602 time.

603

604 An important limitation on long-term reconstructions of NFI plot-level growth arises from  
605 temporal changes in stand conditions (e.g., demography and competition). Specifically, trees  
606 alive at the time of sampling do not necessarily represent a random subset of the trees that  
607 once lived (i.e. the forest composition and characteristics back in time). While random or  
608 systematic sampling avoids the biases associated with the tree-selection principle of  
609 traditional dendroclimatology, other biases remain (e.g., slow-grower survivorship bias or  
610 fading record; Brienen et al., 2012; Swetnam et al., 1999). These pitfalls highlight the merits  
611 of establishing and maintaining permanent NFI remeasurement plots on a multi-decadal scale  
612 that can track temporal changes in stand conditions and complement time-series of climatic  
613 predictors in statistical models. However, most existing NFIs do not yet offer sufficient  
614 temporal depth to account for forest dynamics. One possible solution is to apply the best  
615 available empirical models of stand development (*i.e.*, growth-and-yield models, density  
616 management diagrams, empirical succession mapping) to reconstruct past stand conditions.  
617 Related (Bayesian) approaches may use state data assimilation or a state-space modeling  
618 framework to parameterize models of stand development from experimental forests where

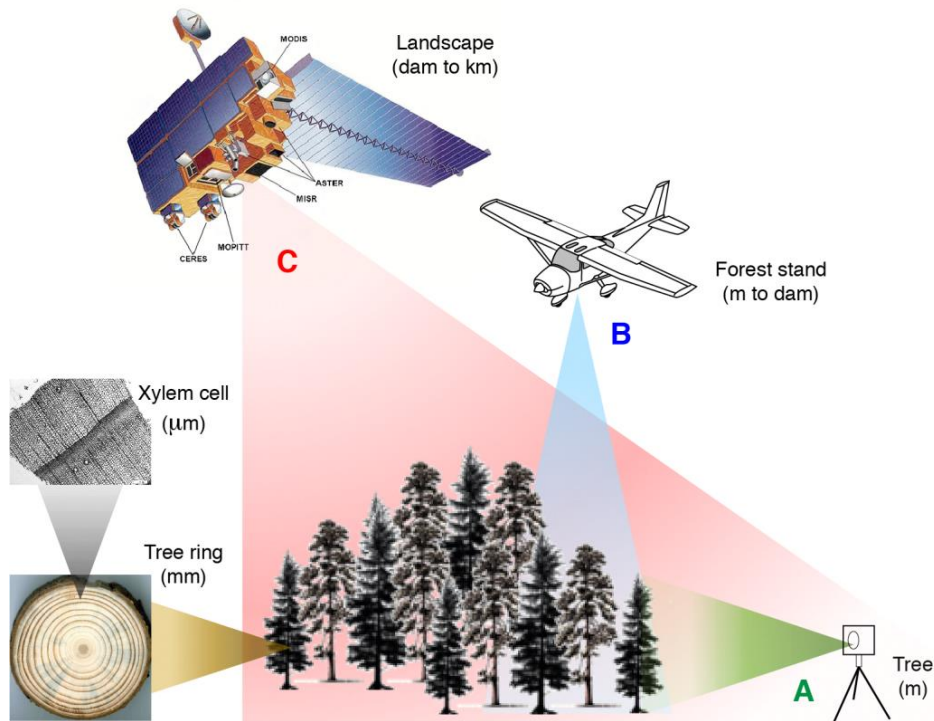
619 data do extend for several decades. Addressing the slow-grower survivorship bias and the  
620 competitive influence of trees that are no longer on the landscape will be crucial to fully  
621 realizing the research potential of paired tree-ring and forest plot data to reconstruct forest  
622 growth in pre-inventory times.

623

### 624 *3.2. Earth observations*

625 Remotely sensed earth observations are a crucial tool for large-scale quantification and  
626 monitoring of ecosystem dynamics across space, and more recently also across time (e.g.  
627 (Zhu et al., 2016). The increasing length of continuous satellite records, e.g. the Landsat Data  
628 Continuity Mission (LDCM), facilitates integration with temporally more coarsely resolved  
629 data such as tree rings (Vicente-Serrano et al., 2016). In addition, we emphasize here that the  
630 combination of tree-ring data with earth observations is not restricted to large-scale  
631 applications, but that it can support and advance all three scaling steps (Figure 5). This is  
632 possible because – independent of the spatial scale – all information derived from remote  
633 sensing systems is fundamentally based on relating spectral reflectance data to field  
634 measurements via empirical models.

635



636

637 **Figure 5:** Overview of the spatial scales at which tree-ring and remotely sensed observations  
 638 can be integrated to support the three upscaling steps (A-C). dam - decameter  
 639

640 Terrestrial light detection and ranging data (LiDAR; also called terrestrial laser scanning,  
 641 TLS) are the remotely sensed data most relevant at the individual tree scale. The application  
 642 of TLS systems to characterize forest stands began about a decade ago (see Newnham et al.,  
 643 2015 for a review) and recent methodological advances have included structural modeling of  
 644 individual trees based on TLS point clouds (Åkerblom et al., 2015). The potential to estimate  
 645 above-ground (and even below-ground; Liski et al., 2014) biomass from such data is  
 646 increasingly explored (Calders et al., 2015). But similar to conventional forest inventory data  
 647 (Section 3.1), TLS does not provide temporal information on tree growth. Hence, the  
 648 integration of tree-ring and TLS data to reconstruct historical tree dimensions (scaling step A,  
 649 Figure 1) is promising, because it helps mitigate uncertainties related to the use of allometric  
 650 functions and may offer a more precise representation of individual tree shapes (Wagner et  
 651 al., 2017). Application of TLS in dense forest stands can, however, be complicated by

652 occlusion effects (e.g. bushes or small trees blocking the view of the scanner), weather  
653 conditions (wind, precipitation, or fog), and limitations of the scanning device itself. The  
654 latter concern is mostly the coarser spatial resolution of distant tree parts (i.e. crowns)  
655 compared to that of lower stem parts, as well as the time it takes to scan an entire forest stand  
656 from a sufficient number of angles to produce a continuous point cloud. Both these  
657 methodological challenges and the expected benefits of integrating TLS data with tree-ring  
658 measurements to produce long-term tree volume reconstructions are yet to be explored.

659

660 Airborne remote sensing is showing the most potential for scaling to the site level (step B,  
661 Figure 1). LiDAR can provide three-dimensional information about vegetation structure at  
662 local to regional scales and structure from motion photogrammetry (Westoby et al., 2012) can  
663 provide approximations thereof. Such information can be calibrated against *in-situ* data of  
664 basal area, canopy height, biomass, stand density, or leaf area to assess spatial variability in  
665 these parameters (Jucker et al., 2017). If repeated LiDAR flights are available, though still  
666 challenging, it is even possible to monitor temporal dynamics in integrated and height-  
667 specific canopy parameters (Griebel et al., 2017). Temporally resolved LiDAR data are still  
668 very rare, but should become more readily available with the increasing use of aircraft  
669 (Cunliffe et al., 2016) and drones (Tang and Shao, 2015) in forest monitoring programs.  
670 Because of the discontinuous data availability in both space and time, integration of airborne  
671 LiDAR with tree-ring records has so far been limited. This link will be strengthened in the  
672 future as advances are made on both sides: tree-ring sampling will become spatially more  
673 representative (Section 3.1); airborne LiDAR will increasingly be used to characterize not  
674 only larger forest stands, but also individual trees (Eysn et al., 2015), which can complement  
675 the application of TLS in complex stands. These efforts are converging towards more precise  
676 estimation and reconstruction of tree- and stand-level biomass and/or basal area increment.

677

678 While integration of tree-ring data with terrestrial and airborne LiDAR is still in its infancy,  
679 combining tree-ring and spectral data from polar-orbiting satellites is well established.  
680 Examples of environmental research that has used this combination include ecology (D'arrigo  
681 et al., 2000; Dorman et al., 2015; Huang et al., 2015), entomology (Çoban et al., 2014;  
682 Sangüesa-Barreda et al., 2014) and hydrology (Morales et al., 2015). For example, tree-ring  
683 data have been used to verify insect defoliation classifications inferred from remote sensing  
684 (Babst et al., 2010; Çoban et al., 2014), or as a proxy to reconstruct inter-annual fluctuations  
685 in lake area observed from Landsat time series (Morales et al., 2015). The satellite-derived  
686 parameter most frequently combined with tree rings has been the Normalized Difference  
687 Vegetation Index (NDVI), a measure of vegetation greenness. With now over thirty years of  
688 repeated observations, global data products such as the Global Inventory for Mapping and  
689 Modeling Studies (GIMMS; Tucker et al., 2005), have allowed for the comparison of tree-  
690 ring and NDVI responses to environmental change across a range of spatial and temporal  
691 scales (Coulthard et al., 2017; Kaufmann et al., 2004; Vicente-Serrano et al., 2013). The most  
692 common approaches have been to either compare the climate signals that are embedded in  
693 these two data streams (Del Castillo et al., 2015; Girardin et al., 2014; Pasho and Alla, 2015),  
694 or to correlate time series of tree rings and NDVI directly (Beck et al., 2013; Berner et al.,  
695 2011; Bunn et al., 2013; D'arrigo et al., 2000; Girardin et al., 2016; Poulter et al., 2013;  
696 Vicente-Serrano et al., 2016). Generally, these studies have found a positive correlation of  
697 moderate strength between inter-annual NDVI variability and annual tree growth. However,  
698 there are notable exceptions along the North American Arctic treeline (Beck et al., 2013), in  
699 Europe (Pasho and Alla, 2015), and in parts of Canada (Girardin et al., 2016) where a  
700 significant positive correlation is not detected. These previous findings point to two main  
701 challenges associated with the integration of tree-ring and satellite observations.

702

703 The first challenge concerns the mismatch in spatial scale between site-level observations of  
704 tree rings and raster data from satellite sensors. The latter integrate surface reflectance  
705 information at various spatial scales, e.g, 30 m for Landsat, 250 m for MODIS, and 1-8 km  
706 for AVHRR. Each pixel integrates a mixture of species, disturbance histories, and land use  
707 activities that may affect the spectral information and complicate the comparison with single-  
708 species tree-ring chronologies. The second challenge emerges from temporal mismatches  
709 between the processes of canopy formation, leaf-level photosynthesis (observed by satellites),  
710 and wood formation (integrated in annual rings) in trees. The climate response of  
711 photosynthesis is more or less instantaneous, but there is a well-documented time lag  
712 between photosynthetic carbon uptake, growth, and biomass increment (Cuny et al., 2015).  
713 Furthermore, it is well known that climate variability can have lagged effects on tree growth  
714 via the storage and remobilization of carbohydrate reserves (Richardson et al., 2013; Zhang et  
715 al., 2017, Fritts, 1976). For all these reasons, tree-ring data and vegetation indices cannot be  
716 expected to fully correspond, and the dynamics of these processes and associated temporal  
717 lags likely differ among ecosystems, species, and climatic domains.

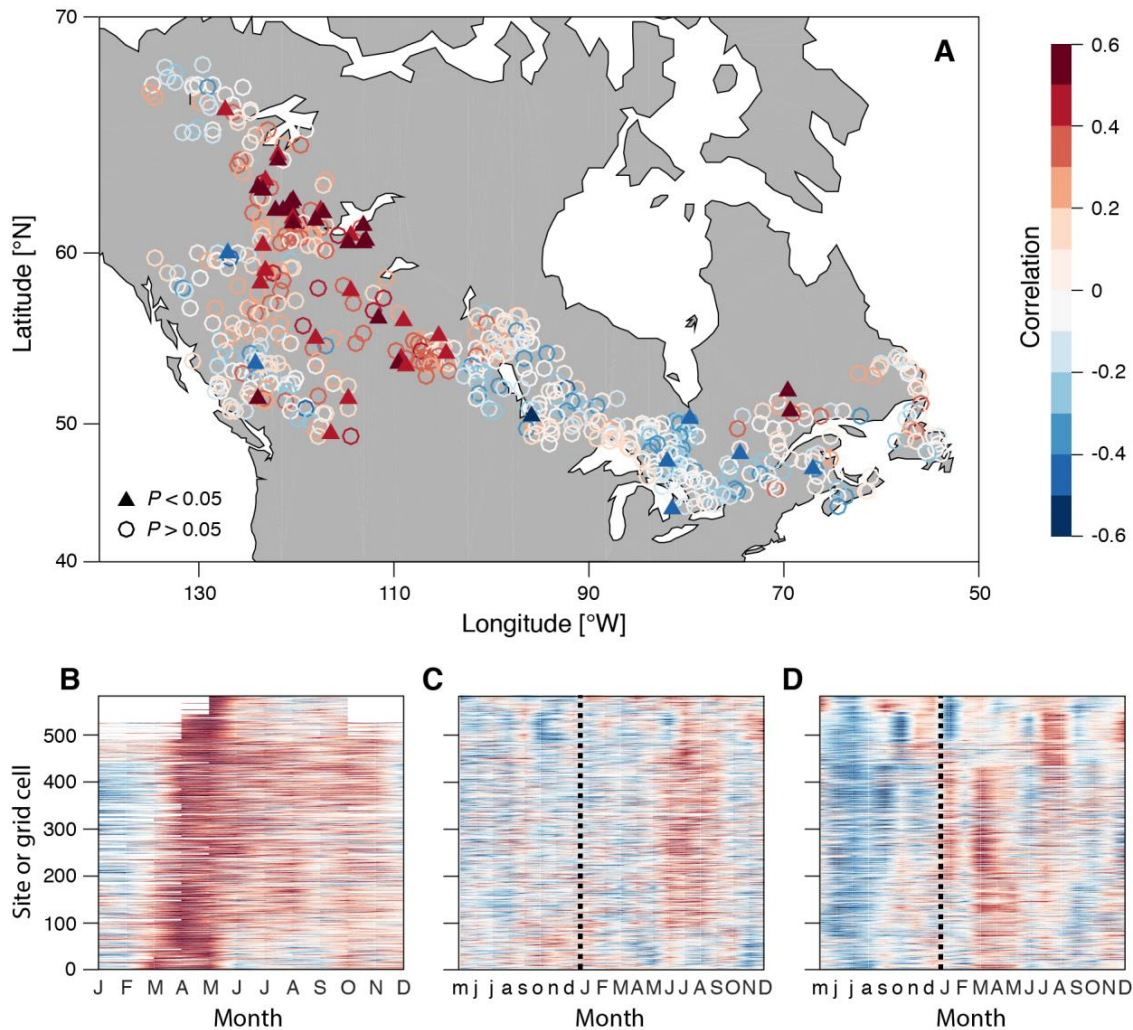
718

### 719 *3.2.1 Practical Example 2: Comparing tree-ring and NDVI data across Canada*

720 To illustrate the temporal mismatch of canopy processes and stem growth, we compared tree-  
721 ring width, NDVI, and their correlations with monthly CRU TS-3.22 temperature (Harris et  
722 al., 2014) from the corresponding grid cells across Canada's boreal forest (Figure 6). We  
723 obtained tree-ring width data from 598 plots (19 species) that were established as part of the  
724 Canadian NFI program. The tree-ring data were detrended using generalized negative  
725 exponential models and whitened (see Girardin et al., 2016 for details). For each plot, we  
726 obtained the corresponding GIMMS-3g NDVI record (Tucker et al., 2005), aggregated into a



727 0.5° regular grid using nearest-neighbor interpolation and subsequently averaged at monthly  
728 resolution. Point-wise Pearson correlations were computed among all three datasets over the  
729 1982-2002 period. This analysis showed that tree-ring width and NDVI correlate in areas  
730 where they are both driven by temperature during the same season (Figure 6). In some areas,  
731 however, the seasonality in the climate response differed clearly between NDVI and tree-ring  
732 width, which may at least partly explain why some studies report a spatially heterogeneous  
733 correlation between the two metrics (Beck et al., 2013; Girardin et al., 2016; Pasho and Alla,  
734 2015). From this example it is evident that spatiotemporal patterns in tree-ring data and  
735 vegetation indices are not equivalent – their representation of different tree organs together  
736 with associated differences in processes and climatic drivers need to be considered in any  
737 comparison.



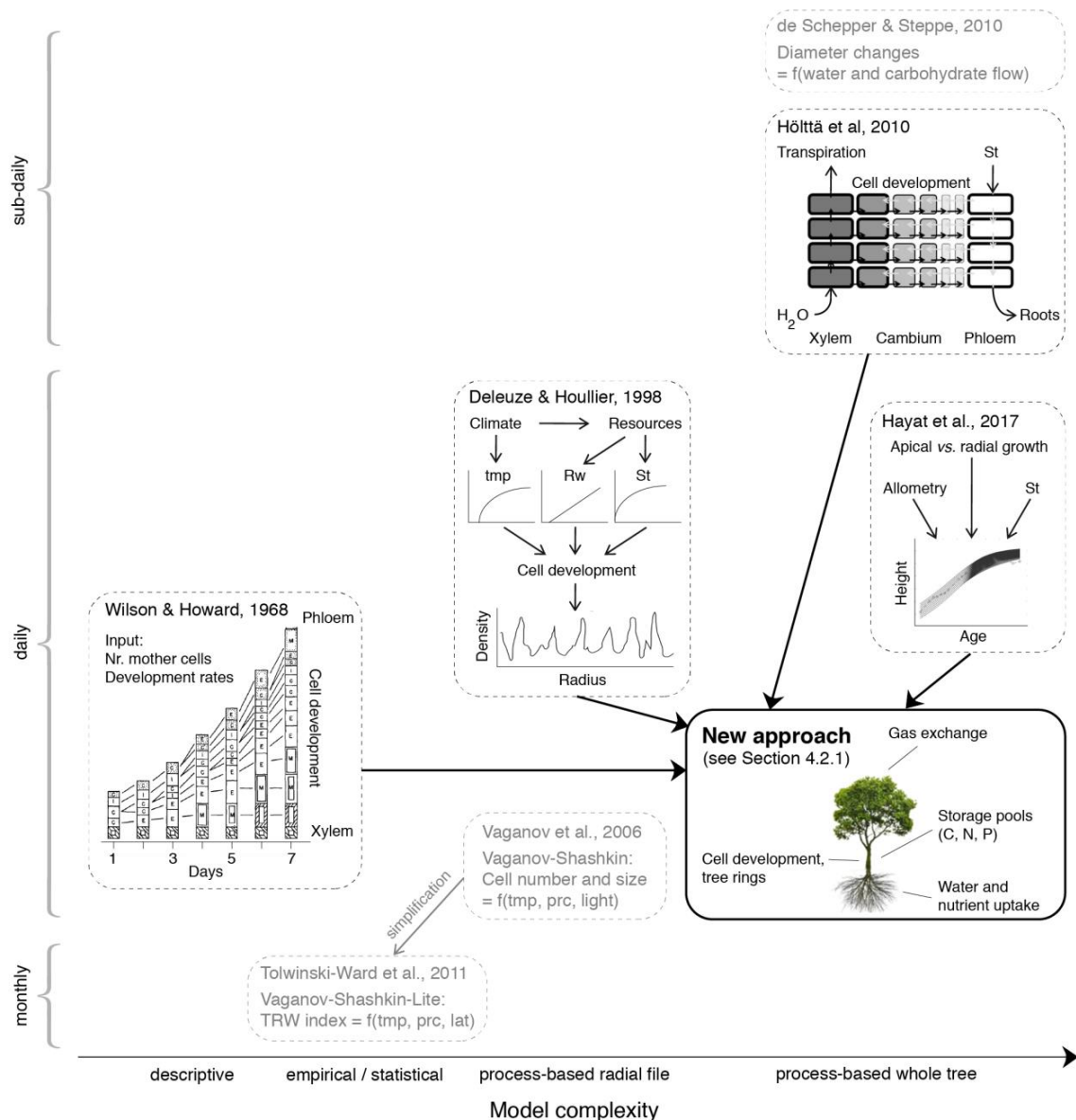
738

739 **Figure 6:** Pearson correlation coefficients between detrended tree-ring width (TRW), the  
 740 normalized difference vegetation index (NDVI), and temperature (tmp) over the 1982-2002  
 741 period. Panel (a): June-August NDVI vs. TRW; Panel (b): NDVI vs. tmp; Panel (c) June-  
 742 August NDVI vs. tmp; Panel (d): TRW vs. tmp. Please note that sites and grid cells are  
 743 ordered by increasing latitude in panels (b-d). Dashed lines separate the previous and current  
 744 year.  
 745

#### 746 4. Mechanistic modeling of tree growth

747 Static statistical relationships derived from observations are clearly limited in terms of  
 748 representing feedbacks in ecosystems (Scholes, 2017), and it is not clear how well these past  
 749 relationships will serve to predict forest responses to the novel conditions in the  
 750 Anthropocene. Hence, there is need to include more process information when linking wood

751 formation to environmental variability, when reconstructing historical climate (Guiot et al.,  
 752 2014), and especially when attempting to forecast into a future time frame (Gustafson, 2013).  
 753 Figure 7 illustrates the current range of tree-ring model complexity, from highly empirical  
 754 monthly time-step approaches (e.g. Tolwinski-Ward et al., 2011) to highly physiological  
 755 simulations of carbon and water flows in whole trees at very fine time steps (De Schepper  
 756 and Steppe, 2010; Hölttä et al., 2010). A new approach is also shown within this scheme,  
 757 with the objective of linking specific cambial-growth and whole-tree physiological models  
 758 for global applications (see Section 4.2.1 for a description).



759

760 **Figure 7:** Models of xylogenesis have been developed at different levels of complexity and  
761 across a range of temporal scales. Efforts are now being made to develop a new and broadly  
762 applicable modeling approach (Section 4.2.1) that will simulate whole tree growth as a  
763 function of environmental influences on physiological processes. Tmp – temperature; prc –  
764 precipitation; lat – latitude; St – photosynthates; Rw – soil moisture  
765

#### 766 *4.1. Simulating radial growth as a function of climatic controls*

767 Wilson and Howard (1968) published the first model of intra-annual xylogenesis, which  
768 reproduced the daily cellular development throughout the growing season using “rules” to  
769 regulate cellular division, enlargement, wall thickening, and death. Realistic daily xylem  
770 development was simulated, but as no environmental controls were imposed (i.e. the rates of  
771 growth processes were model inputs), this approach can be considered “descriptive”. A  
772 handful of models were subsequently published (Howard and Wilson, 1972; Stevens, 1975;  
773 Wilson, 1973) that still required time-varying input parameters to produce realistic growth  
774 rings. To overcome these limitations, Fritts et al. (1991) developed a mechanistic model of  
775 daily cellular development called TRACH that was driven by temperature, water balance, and  
776 day length. This approach was already more general and relatively mechanistic, but it  
777 required as input the number of cells produced during the growing season and did not  
778 consider the supply of growth substrates (see Section 4.2). Expanding upon some of the ideas  
779 in TRACH, the now widely used Vaganov-Shashkin (VS) forward model of tree-ring  
780 formation (Vaganov et al., 2006) was developed. The VS model is built around the  
781 assumption that external multivariate environmental forcing exerts a direct and potentially  
782 non-linear influence on secondary tree growth. Accordingly, tree rings and their internal  
783 structure (e.g. cell number and size) are simulated based on climatic controls on the kinetics  
784 of cell formation (Cuny et al., 2014; Rathgeber et al., 2016). The VS model includes two  
785 basic conditions for the non-linear dependence of wood formation on the environment: the  
786 Principle of Limiting Factor (Fritts, 1976) with respect to daily temperature and soil moisture,

787 and a threshold growth response function to represent the dependence of cell formation on  
788 ambient temperature and soil moisture (Vaganov et al., 2006).

789

790 The output of the VS model includes synthetically generated standardized tree-ring indices  
791 that would be expected if local climate were the only external driver of tree growth. The skill  
792 of the VS model (unless fine-tuned for specific sites) is thereby roughly comparable to that  
793 achieved with statistical transfer function methods commonly applied in dendrochronology  
794 (Cook and Pederson, 2011; Evans et al., 2006). However, the VS model has significant  
795 advantages over purely statistical models in that it provides daily-resolved estimates of  
796 integral growth rates throughout the year and attributes them to different climatic drivers  
797 (Shishov et al., 2016). This greatly facilitates the interpretation of inter- and intra-annual  
798 growth patterns, for instance when capturing a reduction in radial growth rates during  
799 summer drought in Mediterranean areas (Touchan et al., 2012). The applicability of the VS  
800 model has also been demonstrated for other biomes across Asia and North America  
801 (Anchukaitis et al., 2006; Evans et al., 2006; Shi et al., 2008; Zhang et al., 2011).  
802 Comparisons between VS-simulated and observed tree-ring chronologies are particularly  
803 interesting, as they allow assessing whether temporal non-stationarity in climate-growth  
804 relationships arise from climate change alone (Anchukaitis et al., 2006), or from other abiotic  
805 or biotic sources.

806

807 Problematically, it is impractical to upscale site-level chronologies (step C, Figure 1) using  
808 the VS model. This is because not all of the detailed information (more than 40 tunable input  
809 parameters) required to drive the simulation of cell-level processes is available at large spatial  
810 scales. Attempting to facilitate such large-scale application, a numerically more efficient  
811 forward tree-ring model, the Vaganov-Shaskin Lite (VSL), has been developed (Tolwinski-

812 Ward et al., 2011). The VSL model excludes the cell-level processes and has thus been  
813 reduced to a product of three limiting climatic factors: temperature, soil water balance and  
814 solar radiation. Furthermore, it runs on monthly time steps and contains only 12 tunable  
815 parameters. Monthly-resolved climatic input data are broadly available from meteorological  
816 stations and often contain much fewer gaps than daily observations. A disadvantage of this  
817 simplification is that the VSL model cannot resolve sub-monthly growth processes related to,  
818 for example, growth phenology and the formation of “false rings” (Touchan et al., 2012). In  
819 short, the VSL model is widely applicable and has been deemed capable of reproducing the  
820 variability in tree-ring width chronologies from more than 2000 sites on the ITRDB  
821 (Breitenmoser et al., 2014). Moreover, outputs from satellite Earth observations (Section 3.2)  
822 and dynamic global vegetation models (DGVMs; Section 4.3) are often provided at monthly  
823 resolution, making the VSL model a good candidate for pseudo-proxy experiments (Evans et  
824 al., 2013).

825

826 The VS and VSL models have proven valuable to study forest growth responses to climate  
827 variability and change, but they still only include climate variables as input parameters and  
828 do not consider other internal and external drivers of tree growth. The incorporation of the  
829 principle of limiting factors in these models is the primary constraint on their ability to  
830 forecast tree growth and its climate response beyond that of commonly employed statistical  
831 models (Section 2). An interesting prospect is to integrate these VS-type models with  
832 vegetation models that explicitly simulate relevant biological processes such as  
833 photosynthesis, respiration, and resource allocation. For example, Mina et al. (2016)  
834 demonstrated that simulations of stand basal area with the ForClim model (Bugmann, 1996)  
835 could be improved by implementing the seasonal climate response of synthetic tree-ring  
836 chronologies from the VSL model. Such model-model integration approaches appear

837 promising and should be extended to larger scales (e.g., using newly developing NFI  
838 networks; Section 3.1) and a variety of DGVMs.

839

#### 840 *4.2. Towards large-scale modeling of whole-tree growth*

841 Tree rings are increasingly used to study the impacts of environmental change on forest  
842 ecosystems and carbon cycling (Babst et al., 2014a; Babst et al., 2017). For such applications,  
843 it is not sufficient to model only direct climate impacts on radial growth (Section 4.1).  
844 Models need to additionally account for indirect effects of changing external forcing (climate,  
845 CO<sub>2</sub>, etc.) via canopy-level processes (Li et al., 2014). An early example of this is the model  
846 of Deleuze and Houllier (1998) that – similar to the VS model – was also designed to reduce  
847 the parameterization requirements of TRACH and predicts intra-annual wood density profiles  
848 of conifer species. In addition to simulating cambial cell division, enlargement, and wall  
849 thickening as functions of climate, their model assumes that wall thickening is co-limited by  
850 the supply of photosynthates, calculated from temperature and transpiration under the  
851 assumption of fixed foliar mass. This model has been successfully used to study intra-annual  
852 fluctuations in wood density, in combination with a more comprehensive treatment of plant  
853 water and photosynthate transport (Wilkinson et al., 2015). However, the implemented cohort  
854 approach to cellular differentiation limits comparisons with observed radial files (von Arx et  
855 al., 2016) and does not include scaling of radial-file growth to the whole tree.

856

857 Considering other processes and time-scales, (De Schepper and Steppe, 2010) developed a  
858 whole-tree model of reversible (diurnal fluctuations in water content) and irreversible  
859 (structural growth) stem diameter variations, using a very detailed representation of dynamic  
860 water and sugar transport between numerous levels in a tree on a time step of less than one  
861 second. Irreversible radial growth occurs as a function of local turgor and sugar content, but

862 the focus of the model is on reversible changes. (Hölttä et al., 2010) built on this model by  
863 adding cellular-level dynamics and thereby produced a remarkably comprehensive approach  
864 to modeling whole-tree growth, albeit omitting hormonal control. Their approach is very  
865 promising as a detailed physiological treatment and produces interesting conclusions  
866 regarding the effect of tree size on environmental influences. However, photosynthesis and  
867 transpiration are computed off-line, rather than as part of the model simulation, and a very  
868 large number of empirical parameters are required. Furthermore, the high-resolution time-  
869 stepping and consequent computing demands presently limit its application for large-scale  
870 studies of forest-environment interactions. Despite the knowledge of xylogenesis captured by  
871 these models, there is to date no generally applicable approach to modeling whole-tree  
872 growth at large scales. This would require a broadly applicable model structure with a few  
873 key parameter differences between plant functional types (or ideally species), as is currently  
874 implemented for photosynthesis in DGVMs (Section 4.3).

875

#### 876 *4.2.1 Practical example 3: Towards a broadly applicable whole-tree model*

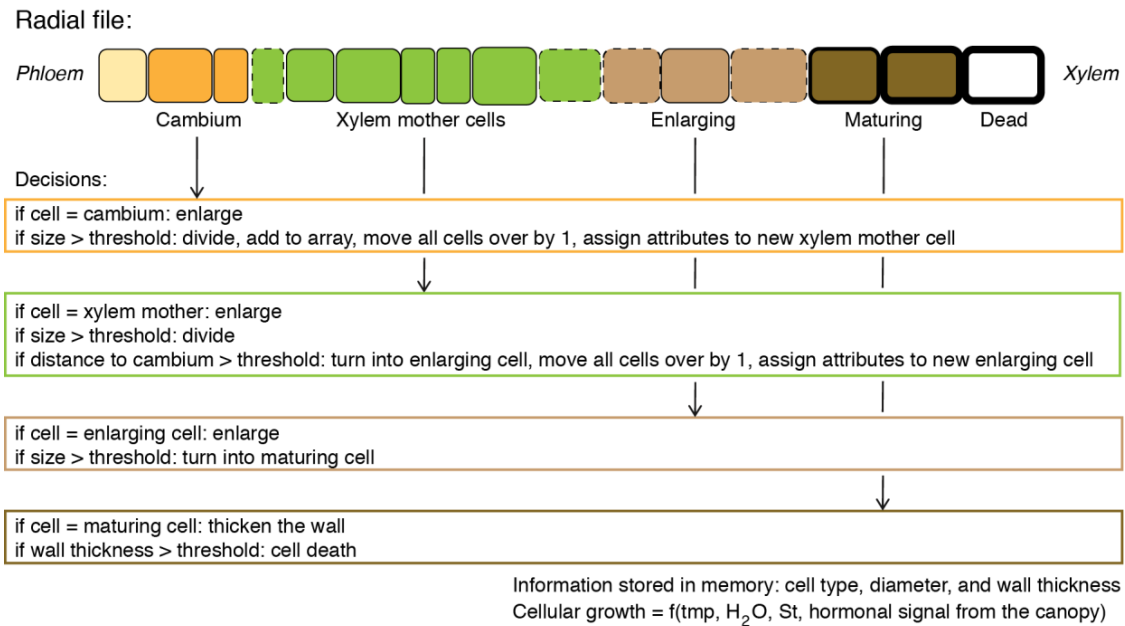
877 Building on the approaches discussed above, a whole-tree model called “Grow\_Up” is  
878 currently being constructed (Friend et al., in prep) that should be capable of being  
879 parameterized for any species and will be incorporated into a DGVM framework. A tree is  
880 assumed to grow as a coordinated whole, led by nutrient uptake and allocation, with foliage  
881 activity promoting cambial growth, resulting in demand for carbon and nutrients from the  
882 developing xylem. Cells in one lateral radial file per tree are represented, with the processes  
883 of division, enlargement, wall thickening, and death controlled by a range of external and  
884 internal factors (Figure 8). The activities of apical meristems are also considered to enable  
885 whole-tree growth as described in (Hayat et al., 2017), an earlier version of this model.  
886 Reserve pools of carbon, nitrogen, and phosphorus enable carry-over effects between years,



887 and the relative activities of the different meristems are controlled by shading, nutrient status,  
888 soil water, and phenological signals.

889

890 Three vectors are used to hold the state variables of the cells in the radial file: the cell  
891 development stage (i.e. cambial initial, xylem mother, enlarging, thickening, or mature),  
892 radial cell diameter, and cell wall thickness. When a cell matures, it is added to the tree stem  
893 and not treated further, although heartwood formation occurs in response to canopy die-back.  
894 The vectors start with the innermost immature cell along the radial file and end at the  
895 innermost phloem mother cell, which is a fixed anchor. The vectors are adjusted as cells are  
896 added through division or lost through maturation. The primary outputs directly derived from  
897 the xylogenetic component of Grow\_Up are annual width and mass increment of the stem, as  
898 well as intra-ring density profiles. More detailed outputs such as the weekly kinetics of  
899 cellular development can also be produced for comparison with observations obtained using  
900 microcores (e.g. Cuny et al., 2014). This basic xylogenetic scheme is assumed to be universal  
901 in all tree species. However, the understanding of the rules governing cambial activation and  
902 dormancy, the rates of cellular division, transitions between cell types, rates of expansion,  
903 and rates of cell wall thickening, is currently incomplete and so the focus is now on testing  
904 various hypotheses.



905

906 **Figure 8:** New model of cell development in a radial file using a vector approach and rules  
907 for cell differentiation based on internal and external drivers. Tmp – temperature; St -  
908 photosynthates

909

910 Initial assumptions for the controls on the development of the radial file assume that the rates  
911 of growth of cambial, mother, and enlarging cells are influenced by water supply,  
912 temperature, a hormonal signal from the canopy, and the concentration of sugars in the  
913 cambium using simple response functions. Cambial cells divide when they reach a critical  
914 size, producing mother cells. Mother cells divide if they reach a critical size and transition to  
915 (non-dividing) enlarging cells when they reach a certain distance from the phloem. Enlarging  
916 cells enter the thickening phase once they reach a critical size, and thickening continues up to  
917 a critical limit at which the cell dies and becomes mature and functional xylem (see Figure 8).

918 The critical cell sizes and cell wall thicknesses, as well as the rates of thickening, are  
919 currently fixed parameters, with only the rates of cellular growth depending on environmental  
920 factors. These assumptions are being tested using microcores collected as components of  
921 various field campaigns and experiments (e.g. Cuny et al., 2014). This scheme is currently  
922 being implemented within the HYBRID9 DGVM framework (a derivative of the model of

923 (Friend, 2010; Friend and White, 2000), and it is anticipated that this new approach will  
924 challenge the predictions of the current generation of DGVMs in fundamental ways, as well  
925 as open them up to direct comparison with tree-ring archives.

926

#### 927 *4.3. Tree-ring integration with ecophysiological and dynamic global vegetation models*

928 Climate policy relies heavily on predictions from earth system models, including their crucial  
929 DGVM sub-components required to model terrestrial carbon fluxes, water exchange, and  
930 energy balances (Boucher et al., 2016). Current DGVMs struggle, however, to simulate forest  
931 growth and its climate response accurately, particularly at annual or longer time scales  
932 (Anderegg et al., 2015; Pappas et al., 2017; Rollinson et al., 2017; Tei et al., 2017; Zhang et  
933 al., 2017). Hence, we see great potential for both tree-ring observations and ecophysiological  
934 models of tree growth to help evaluate and improve DGVMs. A conceptual challenge thereby  
935 is to reconcile the carbon source (i.e. photosynthesis) and sink limitations on tree growth  
936 (Fatichi et al., 2014; Körner, 2015). Sink limitations (see Section 4.1) and their possible  
937 feedbacks on photosynthesis are currently not implemented in DGVMs, which generates  
938 uncertainty (Friend et al., 2014) because growth is treated only as a downstream process.  
939 Explicitly representing xylogenesis in DGVMs (see Section 4.2.1), or at least evaluating  
940 DGVMs at stand and regional scales using ecophysiological models with explicit tree growth  
941 modules, could be a promising way to refine projections of terrestrial carbon cycling. Until  
942 this approach can be fully implemented and rigorously tested, tree rings should continue to be  
943 used in DGVM development by serving as observational references for model-data  
944 comparisons and model parameterization.

945

946 Past research has revealed a large spread in the ability of different DGVMs to reproduce  
947 patterns observed in tree rings. Besides being exceedingly sensitive to climate variability

948 (Rollinson et al., 2017; Zhang et al., 2017; Klesse et al. in review b), modeled NPP tends to  
949 recover much more quickly after extreme events (Anderegg et al., 2015) and lacks the  
950 memory effects that are commonly observed in tree-ring observations also in non-extreme  
951 years (Pappas et al., 2017; Zhang et al., 2017). Accordingly, neither the significant  
952 correlations with previous year's climate, nor the positive auto-correlation structure of most  
953 tree-ring time series are simulated accurately. These findings point to deficits in the carbon  
954 allocation schemes that are implemented in current DGVMs (Sitch et al., 2015). Carbon  
955 allocation and turnover have been identified as an important source of uncertainty (Bloom et  
956 al., 2016; De Kauwe et al., 2014; Friend et al., 2014; Montané et al., 2017) that is  
957 compounded by a shortage of long-term observations of root and foliar dynamics.

958

959 The MAIDEN model (Misson, 2004), an ecophysiological model with a sophisticated carbon  
960 allocation scheme, has shown high correlations ( $r > 0.5$ ) with tree-ring chronologies from  
961 coniferous and broadleaf species at Mediterranean and boreal sites (Gea-Izquierdo et al.,  
962 2015; Gennaretti et al., 2017). MAIDEN uses mechanistic rules for the temporal allocation of  
963 photosynthates to four carbon pools (leaves, stem, roots, and non-structural carbohydrates)  
964 according to phenological phases. While its large-scale application to estimate tree growth is  
965 still limited because certain allocation parameters need to be fitted site-by-site, the integration  
966 of the MAIDEN model with tree-ring observations has already been proposed with a view on  
967 paleo-applications. For instance, (Guiot et al., 2014) have advocated the use of this and other  
968 ecophysiological models in the inverse mode to hindcast climate variability over centuries. In  
969 this application, the model parameters are first manually or automatically optimized to  
970 represent the observed radial increment. Using model-data-fusion techniques (Peng et al.,  
971 2011) the tree-ring data are then assimilated into the model to iteratively constrain the most  
972 likely climate conditions (i.e. probability distributions) that produce the observed radial

973 increment in a given year (Boucher et al., 2014). For the pre-instrumental period when only  
974 tree-ring data are available, the climate probability distribution of a chosen reference (i.e.  
975 average) year is iteratively modified according to the annual tree-ring anomaly for that year  
976 (Guiot et al., 2014). This way, a climate probability distribution for each year of the  
977 reconstruction is determined. Such climate reconstructions based on ecophysiological models  
978 have the advantage over purely empirical calibrations that the influence of non-climatic  
979 effects that are represented in the model (e.g. CO<sub>2</sub>) can be assessed. Additionally,  
980 mechanistic models are positioned to extract climatic information from tree-ring sites located  
981 away from the extreme growth environments typically considered for dendroclimatic  
982 reconstruction. Recalling that classical site selection practices for dendroclimatology were  
983 designed to optimize the signals from a single growth limiting factor (e.g., warm season  
984 temperatures or spring precipitation; see Section 2.1), vast areas where tree growth is  
985 influenced by multiple climatic parameters have remained more moderately utilized and  
986 primarily incorporated in drought reconstructions, whereby drought metrics such as the  
987 Palmer Drought Severity Index and the related tree-ring signals extracted are driven by both  
988 thermal and moisture conditions (e.g. Cook et al., 2015; Cook et al., 2004). Mechanistic  
989 models are positioned to identify separately the precipitation and temperature signals back in  
990 time embedded within tree-ring chronologies with mixed and temporally changing growth  
991 limitations.

992

993 With a view on DGVM development, model-data-fusion approaches involving tree-ring data  
994 (see above) could constrain carbon allocation to stem growth and thereby help evaluate and  
995 improve allocation schemes. In addition, a series of model inter-comparison exercises would  
996 be useful to determine why some models perform better than others in simulating forest  
997 growth and its climate response. Such exercises are being conducted for various ecosystem

998 variables (see e.g. the MsTMIP project of the North American Carbon Program;  
999 <https://nacp.ornl.gov/MsTMIP.shtml>) and we are convinced that including tree-ring  
1000 benchmarks from various ecoregions will be quite fruitful for providing quantitative insight  
1001 in the representation of critical processes in DGVMs. However, one challenge for comparing  
1002 multiple models with tree rings will be to generate parameters that are spatially and  
1003 conceptually comparable. On one hand, estimates of absolute growth rates (e.g. in  $\text{g C m}^{-2}\text{y}^{-1}$ )  
1004 from tree rings facilitate comparisons with standard DGVM output (e.g. net primary  
1005 productivity, in  $\text{g C m}^{-2}\text{y}^{-1}$ ). On the other hand, transforming radial growth into biomass  
1006 increment generates uncertainty (see Section 3.1) that is best avoided if tree-ring data are to  
1007 serve as an observational benchmark. Hence, we advocate that tree-ring width should become  
1008 a standard output parameter (or “emergent property”) of DGVMs and that the detail of the  
1009 implemented carbon pools (leaves, branches, stem, coarse and fine roots, non-structural  
1010 carbohydrates, etc.) in the models be re-examined for comparison with tree rings and other  
1011 ecological data.

1012

### 1013 **5. Perspectives for tree-ring research**

1014 Our discussion around the statistical scaling of tree-ring data in sections 2 and 3 has  
1015 emphasized the need for representative sampling to capture the heterogeneity of forested  
1016 landscapes. The systematic or random distribution of samples along the body of an individual  
1017 tree, of individual trees within a site, and of sites across the landscape will allow for more  
1018 robust past and future projections across the space where observations are sparse or missing.  
1019 In addition, representative sampling of the area covered by the grid cells of raster data  
1020 products should reduce the spatial mismatch between tree-ring data and satellite Earth  
1021 observations or DGVM output. This objective of spatial representativeness is somewhat new  
1022 to the field of dendrochronology. While other disciplines (e.g. ecosystem ecology or forestry)

1023 have a long history of optimizing sampling schemes for spatial or temporal scaling (Scholes,  
1024 2017), these ideas have only recently started to enter the broad scope of tree-ring research  
1025 and require a certain rethinking of established protocols. For example, if tree-ring sampling  
1026 should represent the absolute growth rates of a larger population of trees (e.g. a stand), the  
1027 strength of the common growth variability among trees (traditionally assessed by the mean  
1028 inter-series correlation) and metrics of how well a finite sample represents the theoretical  
1029 population chronology (Expressed Population Signal; Buras, 2017; Cook and Peters, 1997;  
1030 Wigley et al., 1984) are insufficient quality criteria. Hence, new quality criteria as well as  
1031 guidelines for tree-ring sampling need to be established that serve both the needs of  
1032 individual studies and the overarching goal of scaling. We recommend that this be done  
1033 through interdisciplinary research initiatives that involve experts from complimentary  
1034 disciplines, including dendrochronology, forest and landscape ecology, forestry, and  
1035 statistical ecology.

1036

1037 At present, we have the best understanding of uncertainties in tree-ring data at the site level.  
1038 Over the past years, a number of studies have characterized trend biases in time series of tree  
1039 growth (e.g. Brienen et al., 2012; Brienen et al., 2017; Peters et al., 2015) or the impact of  
1040 sampling practices on tree-ring quantification of stand-level above-ground biomass increment  
1041 (Alexander et al., 2017; Nehrbass - Ahles et al., 2014). These studies will serve as important  
1042 guidelines in future field campaigns. In contrast, sampling biases at the individual level are  
1043 insufficiently constrained, especially when the goal is to represent full stem or tree-level  
1044 growth. This is in part because the heterogeneity and dynamics of resource allocation to stem  
1045 growth are not well understood. This could for example be tackled through intense sampling  
1046 along trees that were commercially felled or uprooted after a storm. If combined with wood  
1047 anatomical measurements (von Arx et al., 2016), such data could additionally serve as an

1048 improved test bed for mechanistic models of xylogenesis (Section 4). These models are  
1049 becoming increasingly important tools to assess, reconstruct, and forecast tree growth  
1050 responses to a changing environment because – even with the most representative sampling –  
1051 statistical scaling is challenged by feedbacks in ecosystem processes (Scholes, 2017). Finally,  
1052 uncertainties in tree-ring data will be the most challenging to assess at large spatial scales  
1053 where individual- and site-level uncertainties cumulate and where the number of existing  
1054 records may not suffice to counteract uncertainty from spatial heterogeneity. Yet, as new  
1055 tree-ring and NFI data with well-quantified uncertainty are made accessible and interoperable  
1056 across national boundaries, a global network of annually resolved forest biomass  
1057 reconstructions can emerge. An important application of these data will then be to evaluate  
1058 the ITRDB and ensure that this legacy of decades of tree-ring research can continue to  
1059 support earth system science (Babst et al., 2017).

1060

1061 When tree rings go global – as is the theme of this review – the goal is to generate knowledge  
1062 and data that can inform adaptation and mitigation strategies in the face of climate change.  
1063 The primary strength of tree-ring records has so far been seen in their temporal depth that  
1064 allows placing the current climatic variability and ongoing trends in a millennium-length  
1065 context. Indeed, it is both important and disturbing to learn that the Earth is warming at an  
1066 unprecedented rate (Esper et al., 2018; Wilson et al., 2016), that man-made influences on  
1067 atmospheric circulation patterns can promote more frequent extreme events (e.g. through  
1068 Arctic warming; (Trouet et al., 2018), and that these events are directly linked to forest  
1069 mortality, disturbances, and changes in the terrestrial carbon cycle (Schwalm et al., 2017;  
1070 Schwalm et al., 2012; Williams et al., 2013). However, anthropogenic climate change is now  
1071 considered indisputable and there is a need to transition towards tree-ring research that  
1072 assesses, reconstructs and projects the responses and feedbacks of forest ecosystems to



1073 climate change. Dendrochronology can make important contributions at every step of  
1074 successful scaling (Sections 2 and 3) and refined process understanding (Section 4). How and  
1075 how quickly can we expect tree growth and its climate sensitivity to change with continued  
1076 warming? Will thinning forests mitigate drought stress? How much carbon will be  
1077 sequestered by forests under various management scenarios? By answering these and other  
1078 relevant questions, tree-ring research can directly support the development and assessment of  
1079 climate change adaptation strategies.

1080

### 1081 **Acknowledgements**

1082 F.B. acknowledges funding from the EU-H2020 program (grant 640176, “BACI”) and the  
1083 Swiss National Science Foundation (#P300P2\_154543). S.K. acknowledges the support of  
1084 the USDA-AFRI grant 2016-67003-24944. A.D.F and R.H.T acknowledge support from the  
1085 Natural Environment Research Council through grant number NE/P011462/1.

### 1086 **References**

1087 Adams, H.D., Zeppel, M.J., Anderegg, W.R., Hartmann, H., Landhäusser, S.M., Tissue, D.T.,  
1088 Huxman, T.E., Hudson, P.J., Franz, T.E., Allen, C.D., 2017. A multi-species synthesis of  
1089 physiological mechanisms in drought-induced tree mortality. *Nature ecology & evolution*  
1090 1, 1285.  
1091 Ainsworth, E.A., Long, S.P., 2005. What have we learned from 15 years of free - air CO<sub>2</sub>  
1092 enrichment (FACE)? A meta - analytic review of the responses of photosynthesis, canopy  
1093 properties and plant production to rising CO<sub>2</sub>. *New Phytologist* 165, 351-372.  
1094 Aitken, S.N., Yeaman, S., Holliday, J.A., Wang, T., Curtis - McLane, S., 2008. Adaptation,  
1095 migration or extirpation: climate change outcomes for tree populations. *Evolutionary*  
1096 *Applications* 1, 95-111.  
1097 Åkerblom, M., Raunonen, P., Kaasalainen, M., Casella, E., 2015. Analysis of geometric  
1098 primitives in quantitative structure models of tree stems. *Remote Sensing* 7, 4581-4603.  
1099 Alexander, M.R., Rollinson, C.R., Babst, F., Trouet, V., Moore, D.J., 2017. Relative  
1100 influences of multiple sources of uncertainty on cumulative and incremental tree-ring-  
1101 derived aboveground biomass estimates. *Trees*, 1-12.  
1102 Anchukaitis, K.J., Evans, M.N., Kaplan, A., Vaganov, E.A., Hughes, M.K., Grissino-Mayer,  
1103 H.D., Cane, M.A., 2006. Forward modeling of regional scale tree-ring patterns in the  
1104 southeastern United States and the recent influence of summer drought. *Geophysical*  
1105 *Research Letters* 33.

- 1106 Anderegg, W.R.L., Schwalm, C., Biondi, F., Camarero, J.J., Koch, G., Litvak, M., Ogle, K.,  
1107 Shaw, J.D., Shevliakova, E., Williams, A.P., Wolf, A., Ziaco, E., Pacala, S., 2015.  
1108 Pervasive drought legacies in forest ecosystems and their implications for carbon cycle  
1109 models. *Science* 349, 528-532.
- 1110 Babst, F., Alexander, M.R., Szejner, P., Bouriaud, O., Klesse, S., Roden, J., Ciais, P., Poulter,  
1111 B., Frank, D., Moore, D.J., 2014a. A tree-ring perspective on the terrestrial carbon cycle.  
1112 *Oecologia* 176, 307-322.
- 1113 Babst, F., Bouriaud, O., Alexander, R., Trouet, V., Frank, D., 2014b. Toward consistent  
1114 measurements of carbon accumulation: A multi-site assessment of biomass and basal area  
1115 increment across Europe. *Dendrochronologia* 32, 153-161.
- 1116 Babst, F., Esper, J., Parlow, E., 2010. Landsat TM/ETM+ and tree-ring based assessment of  
1117 spatiotemporal patterns of the autumnal moth (*Epirrita autumnata*) in northernmost  
1118 Fennoscandia. *Remote Sensing of Environment* 114, 637-646.
- 1119 Babst, F., Poulter, B., Bodesheim, P., Mahecha, M.D., Frank, D.C., 2017. Improved tree-ring  
1120 archives will support earth-system science. *Nature Ecology & Evolution* 1, 0008.
- 1121 Babst, F., Poulter, B., Trouet, V., Tan, K., Neuwirth, B., Wilson, R., Carrer, M., Grabner, M.,  
1122 Tegel, W., Levanic, T., 2013. Site - and species - specific responses of forest growth to  
1123 climate across the European continent. *Global Ecology and Biogeography* 22, 706-717.
- 1124 Bakker, J.D., 2005. A new, proportional method for reconstructing historical tree diameters.  
1125 *Canadian Journal of Forest Research-Revue Canadienne De Recherche Forestiere* 35,  
1126 2515-2520.
- 1127 Bechtold, W.A., Patterson, P.L., 2005. The enhanced forest inventory and analysis program-  
1128 national sampling design and estimation procedures. Gen. Tech. Rep. SRS-80. Asheville,  
1129 NC: US Department of Agriculture, Forest Service, Southern Research Station. 85 p. 80.
- 1130 Beck, P.S., Andreu-Hayles, L., D'Arrigo, R., Anchukaitis, K.J., Tucker, C.J., Pinzón, J.E.,  
1131 Goetz, S.J., 2013. A large-scale coherent signal of canopy status in maximum latewood  
1132 density of tree rings at arctic treeline in North America. *Global and planetary change* 100,  
1133 109-118.
- 1134 Berner, L.T., Beck, P.S., Bunn, A.G., Lloyd, A.H., Goetz, S.J., 2011. High - latitude tree  
1135 growth and satellite vegetation indices: Correlations and trends in Russia and Canada  
1136 (1982-2008). *Journal of Geophysical Research: Biogeosciences* 116.
- 1137 Björklund, J., Seftigen, K., Schweingruber, F., Fonti, P., Arx, G., Bryukhanova, M.V., Cuny,  
1138 H.E., Carrer, M., Castagneri, D., Frank, D.C., 2017. Cell size and wall dimensions drive  
1139 distinct variability of earlywood and latewood density in Northern Hemisphere conifers.  
1140 *New Phytologist* 216, 728-740.
- 1141 Black, B.A., Griffin, D., Sleen, P., Wanamaker, A.D., Speer, J.H., Frank, D.C., Stahle, D.W.,  
1142 Pederson, N., Copenheaver, C.A., Trouet, V., 2016. The value of crossdating to retain  
1143 high - frequency variability, climate signals, and extreme events in environmental proxies.  
1144 *Global change biology* 22, 2582-2595.
- 1145 Bloom, A.A., Exbrayat, J.-F., van der Velde, I.R., Feng, L., Williams, M., 2016. The decadal  
1146 state of the terrestrial carbon cycle: Global retrievals of terrestrial carbon allocation, pools,  
1147 and residence times. *Proceedings of the National Academy of Sciences* 113, 1285-1290.
- 1148 Boucher, É., Guiot, J., Hatté, C., Daux, V., Danis, P.-A., Dussouillez, P., 2014. An inverse  
1149 modeling approach for tree-ring-based climate reconstructions under changing  
1150 atmospheric CO<sub>2</sub> concentrations. *Biogeosciences* 11, 3245.
- 1151 Boucher, O., Bellassen, V., Benveniste, H., Ciais, P., Criqui, P., Guivarch, C., Le Treut, H.,  
1152 Mathy, S., Séférian, R., 2016. Opinion: In the wake of Paris Agreement, scientists must  
1153 embrace new directions for climate change research. *Proceedings of the National*  
1154 *Academy of Sciences* 113, 7287-7290.

1155 Bouriaud, O., Marin, G., Bouriaud, L., Hessenmöller, D., Schulze, E.-D., 2016. Romanian  
1156 legal management rules limit wood production in Norway spruce and beech forests. *Forest*  
1157 *Ecosystems* 3, 20.

1158 Bouriaud, O., Teodosiu, M., Kirilyanov, A., Wirth, C., 2015. Influence of wood density in  
1159 tree-ring based annual productivity assessments and its errors in Norway spruce.

1160 Breiman, L., 2001. *Random Forest*, 45, 5-32. Examples.

1161 Breitenmoser, P., Brönnimann, S., Frank, D., 2014. Forward modelling of tree-ring width and  
1162 comparison with a global network of tree-ring chronologies. *Climate of the Past* 10, 437-  
1163 449.

1164 Brienen, R.J., Gloor, E., Zuidema, P.A., 2012. Detecting evidence for CO<sub>2</sub> fertilization from  
1165 tree ring studies: The potential role of sampling biases. *Global Biogeochemical Cycles* 26.

1166 Brienen, R.J., Gloor, M., Ziv, G., 2017. Tree demography dominates long - term growth  
1167 trends inferred from tree rings. *Global change biology* 23, 474-484.

1168 Brienen, R.J., Schöngart, J., Zuidema, P.A., 2016. Tree rings in the tropics: insights into the  
1169 ecology and climate sensitivity of tropical trees, *Tropical Tree Physiology*. Springer, pp.  
1170 439-461.

1171 Brzostek, E.R., Dragoni, D., Schmid, H.P., Rahman, A.F., Sims, D., Wayson, C.A., Johnson,  
1172 D.J., Phillips, R.P., 2014. Chronic water stress reduces tree growth and the carbon sink of  
1173 deciduous hardwood forests. *Global Change Biology* 20, 2531-2539.

1174 Buchwal, A., Rachlewicz, G., Fonti, P., Cherubini, P., Gärtner, H., 2013. Temperature  
1175 modulates intra-plant growth of *Salix polaris* from a high Arctic site (Svalbard). *Polar*  
1176 *Biology* 36, 1305-1318.

1177 Buechling, A., Martin, P.H., Canham, C.D., 2017. Climate and competition effects on tree  
1178 growth in Rocky Mountain forests. *Journal of Ecology*.

1179 Bugmann, H.K., 1996. A simplified forest model to study species composition along climate  
1180 gradients. *Ecology* 77, 2055-2074.

1181 Bunn, A.G., Hughes, M.K., Kirilyanov, A.V., Losleben, M., Shishov, V.V., Berner, L.T.,  
1182 Oltchev, A., Vaganov, E.A., 2013. Comparing forest measurements from tree rings and a  
1183 space-based index of vegetation activity in Siberia. *Environmental Research Letters* 8,  
1184 035034.

1185 Buras, A., 2017. A comment on the expressed population signal. *Dendrochronologia* 44, 130-  
1186 132.

1187 Buras, A., van der Maaten-Theunissen, M., van der Maaten, E., Ahlgrimm, S., Hermann, P.,  
1188 Simard, S., Heinrich, I., Helle, G., Unterseher, M., Schnittler, M., 2016. Tuning the Voices  
1189 of a Choir: Detecting Ecological Gradients in Time-Series Populations. *PloS one* 11,  
1190 e0158346.

1191 Calders, K., Newnham, G., Burt, A., Murphy, S., Raunonen, P., Herold, M., Culvenor, D.,  
1192 Avitabile, V., Disney, M., Armston, J., 2015. Nondestructive estimates of above - ground  
1193 biomass using terrestrial laser scanning. *Methods in Ecology and Evolution* 6, 198-208.

1194 Charney, N.D., Babst, F., Poulter, B., Record, S., Trouet, V.M., Frank, D., Enquist, B.J.,  
1195 Evans, M.E., 2016. Observed forest sensitivity to climate implies large changes in 21st  
1196 century North American forest growth. *Ecology letters* 19, 1119-1128.

1197 Charru, M., Seynave, I., Hervé, J.-C., Bertrand, R., Bontemps, J.-D., 2017. Recent growth  
1198 changes in Western European forests are driven by climate warming and structured across  
1199 tree species climatic habitats. *Annals of Forest Science* 74, 33.

1200 Chen, H.Y., Luo, Y., Reich, P.B., Searle, E.B., Biswas, S.R., 2016. Climate change -  
1201 associated trends in net biomass change are age dependent in western boreal forests of  
1202 Canada. *Ecology letters* 19, 1150-1158.

1203 Chhin, S., Hogg, E., Lieffers, V.J., Huang, S., 2010. Growth-climate relationships vary with  
1204 height along the stem in lodgepole pine. *Tree physiology* 30, 335-345.

- 1205 Clark, J.S., Iverson, L., Woodall, C.W., Allen, C.D., Bell, D.M., Bragg, D.C., D'amato, A.W.,  
1206 Davis, F.W., Hersh, M.H., Ibanez, I., 2016. The impacts of increasing drought on forest  
1207 dynamics, structure, and biodiversity in the United States. *Global change biology* 22,  
1208 2329-2352.
- 1209 Clark, J.S., Wolosin, M., Dietze, M., Ibáñez, I., LaDeau, S., Welsh, M., Kloeppel, B., 2007.  
1210 Tree growth inference and prediction from diameter censuses and ring widths. *Ecological*  
1211 *Applications* 17, 1942-1953.
- 1212 Clough, B.J., Curzon, M.T., Domke, G.M., Russell, M.B., Woodall, C.W., 2017. Climate -  
1213 driven trends in stem wood density of tree species in the eastern United States: Ecological  
1214 impact and implications for national forest carbon assessments. *Global Ecology and*  
1215 *Biogeography* 26, 1153-1164.
- 1216 Çoban, H.O., Özçelik, R., Avci, M., 2014. Monitoring of damage from cedar shoot moth  
1217 *Dichelia cedricola* Diakonoff (Lep.: Tortricidae) by multi-temporal Landsat imagery.  
1218 *iForest-Biogeosciences and Forestry* 7, 126.
- 1219 Cook, E.R., 1987. The decomposition of tree-ring series for environmental studies. *Tree-Ring*  
1220 *Bulletin*.
- 1221 Cook, E.R., Briffa, K.R., Meko, D.M., Graybill, D.A., Funkhouser, G., 1995. THE  
1222 SEGMENT LENGTH CURSE IN LONG TREE-RING CHRONOLOGY  
1223 DEVELOPMENT FOR PALEOCLIMATIC STUDIES. *Holocene* 5, 229-237.
- 1224 Cook, E.R., Glitzenstein, J.S., Krusic, P.J., Harcombe, P.A., 2001. Identifying functional  
1225 groups of trees in west Gulf Coast forests (USA): A tree-ring approach. *Ecological*  
1226 *Applications* 11, 883-903.
- 1227 Cook, E.R., Pederson, N., 2011. Uncertainty, emergence, and statistics in dendrochronology,  
1228 *Dendroclimatology*. Springer, pp. 77-112.
- 1229 Cook, E.R., Peters, K., 1997. Calculating unbiased tree-ring indices for the study of climatic  
1230 and environmental change. *Holocene* 7, 361-370.
- 1231 Cook, E.R., Seager, R., Kushnir, Y., Briffa, K.R., Büntgen, U., Frank, D., Krusic, P.J., Tegel,  
1232 W., van der Schrier, G., Andreu-Hayles, L., 2015. Old World megadroughts and pluvials  
1233 during the Common Era. *Science Advances* 1, e1500561.
- 1234 Cook, E.R., Woodhouse, C.A., Eakin, C.M., Meko, D.M., Stahle, D.W., 2004. Long-term  
1235 aridity changes in the western United States. *Science* 306, 1015-1018.
- 1236 Coulthard, B.L., Touchan, R., Anchukaitis, K.J., Meko, D.M., Sivrikaya, F., 2017. Tree  
1237 growth and vegetation activity at the ecosystem-scale in the eastern Mediterranean.  
1238 *Environmental Research Letters* 12, 084008.
- 1239 Cunliffe, A.M., Brazier, R.E., Anderson, K., 2016. Ultra-fine grain landscape-scale  
1240 quantification of dryland vegetation structure with drone-acquired structure-from-motion  
1241 photogrammetry. *Remote Sensing of Environment* 183, 129-143.
- 1242 Cuny, H.E., Rathgeber, C.B., Frank, D., Fonti, P., Fournier, M., 2014. Kinetics of tracheid  
1243 development explain conifer tree - ring structure. *New Phytologist* 203, 1231-1241.
- 1244 Cuny, H.E., Rathgeber, C.B.K., Frank, D., Fonti, P., Mäkinen, H., Prislan, P., Rossi, S., del  
1245 Castillo, E.M., Campelo, F., Vavrčík, H., Camarero, J.J., Bryukhanova, M.V., Jyske, T.,  
1246 Gričar, J., Gryc, V., De Luis, M., Vieira, J., Čufar, K., Kirilyanov, A.V., Oberhuber, W.,  
1247 Treml, V., Huang, J.-G., Li, X., Swidrak, I., Deslauriers, A., Liang, E., Nöjd, P., Gruber,  
1248 A., Nabais, C., Morin, H., Krause, C., King, G., Fournier, M., 2015. Woody biomass  
1249 production lags stem-girth increase by over one month in coniferous forests. 1, 15160.
- 1250 D'arrigo, R., Malmstrom, C., Jacoby, G., Los, S., Bunker, D., 2000. Correlation between  
1251 maximum latewood density of annual tree rings and NDVI based estimates of forest  
1252 productivity. *International Journal of Remote Sensing* 21, 2329-2336.

1253 D'Orangeville, L., Duchesne, L., Houle, D., Kneeshaw, D., Côté, B., Pederson, N., 2016.  
1254 Northeastern North America as a potential refugium for boreal forests in a warming  
1255 climate. *Science* 352, 1452-1455.

1256 Davis, S.C., Hessl, A.E., Scott, C.J., Adams, M.B., Thomas, R.B., 2009. Forest carbon  
1257 sequestration changes in response to timber harvest. *Forest Ecology and Management* 258,  
1258 2101-2109.

1259 De Kauwe, M.G., Medlyn, B.E., Zaehle, S., Walker, A.P., Dietze, M.C., Wang, Y.P., Luo,  
1260 Y., Jain, A.K., El - Masri, B., Hickler, T., 2014. Where does the carbon go? A model-data  
1261 intercomparison of vegetation carbon allocation and turnover processes at two temperate  
1262 forest free - air CO<sub>2</sub> enrichment sites. *New Phytologist* 203, 883-899.

1263 de Rigo, D., Caudullo, G., Houston Durrant, T., San-Miguel-Ayanz, J., 2016. The European  
1264 Atlas of Forest Tree Species: modelling, data and information on forest tree species.  
1265 European Atlas of Forest Tree Species. Publ. Off. EU, Luxembourg, pp. e01aa69+  
1266 <https://w3id.org/mtv/FISE-Comm/v01/e01aa69> (Cited on pages 3, 11, and 28).

1267 De Schepper, V., Steppe, K., 2010. Development and verification of a water and sugar  
1268 transport model using measured stem diameter variations. *Journal of Experimental Botany*  
1269 61, 2083-2099.

1270 Del Castillo, J., Voltas, J., Ferrio, J.P., 2015. Carbon isotope discrimination, radial growth,  
1271 and NDVI share spatiotemporal responses to precipitation in Aleppo pine. *Trees* 29, 223-  
1272 233.

1273 Deleuze, C., Houllier, F., 1998. A simple process-based xylem growth model for describing  
1274 wood microdensitometric profiles. *Journal of Theoretical Biology* 193, 99-113.

1275 DeRose, R.J., Shaw, J.D., Long, J.N., 2017. Building the forest inventory and analysis tree-  
1276 ring data set. *Journal of Forestry* 115, 283-291.

1277 Dorman, M., Svoray, T., Perevolotsky, A., Moshe, Y., Sarris, D., 2015. What determines tree  
1278 mortality in dry environments? a multi - perspective approach. *Ecological Applications*  
1279 25, 1054-1071.

1280 Duchesne, L., D'Orangeville, L., Ouimet, R., Houle, D., Kneeshaw, D., 2017. Extracting  
1281 coherent tree-ring climatic signals across spatial scales from extensive forest inventory  
1282 data. *PloS one* 12, e0189444.

1283 Esper, J., Buntgen, U., Frank, D.C., Nievergelt, D., Liebhold, A., 2007. 1200 years of regular  
1284 outbreaks in alpine insects. *Proceedings of the Royal Society B-Biological Sciences* 274,  
1285 671-679.

1286 Esper, J., George, S.S., Anchukaitis, K., D'Arrigo, R., Ljungqvist, F., Luterbacher, J.,  
1287 Schneider, L., Stoffel, M., Wilson, R., Büntgen, U., 2018. Large-scale, millennial-length  
1288 temperature reconstructions from tree-rings. *Dendrochronologia*.

1289 Evans, M.E., Falk, D.A., Arizpe, A., Swetnam, T.L., Babst, F., Holsinger, K.E., 2017. Fusing  
1290 tree - ring and forest inventory data to infer influences on tree growth. *Ecosphere* 8.

1291 Evans, M.N., Reichert, B.K., Kaplan, A., Anchukaitis, K.J., Vaganov, E.A., Hughes, M.K.,  
1292 Cane, M.A., 2006. A forward modeling approach to paleoclimatic interpretation of tree-  
1293 ring data. *Journal of Geophysical Research-Biogeosciences* 111.

1294 Evans, M.N., Tolwinski-Ward, S.E., Thompson, D.M., Anchukaitis, K.J., 2013. Applications  
1295 of proxy system modeling in high resolution paleoclimatology. *Quaternary Science*  
1296 *Reviews* 76, 16-28.

1297 Eysn, L., Hollaus, M., Lindberg, E., Berger, F., Monnet, J.-M., Dalponte, M., Kobal, M.,  
1298 Pellegrini, M., Lingua, E., Mongus, D., 2015. A benchmark of lidar-based single tree  
1299 detection methods using heterogeneous forest data from the alpine space. *Forests* 6, 1721-  
1300 1747.

1301 Farrior, C.E., Rodriguez-Iturbe, I., Dybzinski, R., Levin, S.A., Pacala, S.W., 2015. Decreased  
1302 water limitation under elevated CO<sub>2</sub> amplifies potential for forest carbon sinks.  
1303 Proceedings of the National Academy of Sciences 112, 7213-7218.

1304 Fatichi, S., Leuzinger, S., Körner, C., 2014. Moving beyond photosynthesis: from carbon  
1305 source to sink - driven vegetation modeling. *New Phytologist* 201, 1086-1095.

1306 Forrester, D.I., Tachauer, I., Annighoefer, P., Barbeito, I., Pretzsch, H., Ruiz-Peinado, R.,  
1307 Stark, H., Vacchiano, G., Zlatanov, T., Chakraborty, T., 2017. Generalized biomass and  
1308 leaf area allometric equations for European tree species incorporating stand structure, tree  
1309 age and climate. *Forest Ecology and Management* 396, 160-175.

1310 Foster, J.R., Finley, A.O., D'amato, A.W., Bradford, J.B., Banerjee, S., 2016. Predicting tree  
1311 biomass growth in the temperate-boreal ecotone: Is tree size, age, competition, or climate  
1312 response most important? *Global change biology* 22, 2138-2151.

1313 Frank, D., Poulter, B., Saurer, M., Esper, J., Huntingford, C., Helle, G., Treydte, K.,  
1314 Zimmermann, N., Schleser, G., Ahlström, A., 2015. Water-use efficiency and transpiration  
1315 across European forests during the Anthropocene. *Nature Climate Change* 5, 579-583.

1316 Friend, A.D., 2010. Terrestrial plant production and climate change. *Journal of experimental  
1317 botany* 61, 1293-1309.

1318 Friend, A.D., Lucht, W., Rademacher, T.T., Keribin, R., Betts, R., Cadule, P., Ciais, P.,  
1319 Clark, D.B., Dankers, R., Falloon, P.D., 2014. Carbon residence time dominates  
1320 uncertainty in terrestrial vegetation responses to future climate and atmospheric CO<sub>2</sub>.  
1321 Proceedings of the National Academy of Sciences 111, 3280-3285.

1322 Friend, A.D., White, A., 2000. Evaluation and analysis of a dynamic terrestrial ecosystem  
1323 model under preindustrial conditions at the global scale. *Global Biogeochemical Cycles*  
1324 14, 1173-1190.

1325 Fritts, H.C., 1976. *Tree Rings and Climate*. The Blackburn Press, Caldwell.

1326 Fritts, H.C., Vaganov, E.A., Sviderskaya, I.V., Shashkin, A.V., 1991. Climatic variation and  
1327 tree-ring structure in conifers: empirical and mechanistic models of tree-ring width,  
1328 number of cells, cell size, cell-wall thickness and wood density. *Climate Research*, 97-  
1329 116.

1330 Galiano, L., Martínez-Vilalta, J., Sabaté, S., Lloret, F., 2012. Determinants of drought effects  
1331 on crown condition and their relationship with depletion of carbon reserves in a  
1332 Mediterranean holm oak forest. *Tree physiology* 32, 478-489.

1333 Gea-Izquierdo, G., Guibal, F., Joffre, R., Ourcival, J., Simioni, G., Guiot, J., 2015. Modelling  
1334 the climatic drivers determining photosynthesis and carbon allocation in evergreen  
1335 Mediterranean forests using multiproxy long time series. *Biogeosciences* 12, 3695-3712.

1336 Gedalof, Z.e., Berg, A.A., 2010. Tree ring evidence for limited direct CO<sub>2</sub> fertilization of  
1337 forests over the 20th century. *Global Biogeochemical Cycles* 24.

1338 Gennaretti, F., Gea-Izquierdo, G., Boucher, E., Berninger, F., Arseneault, D., Guiot, J., 2017.  
1339 Ecophysiological modeling of photosynthesis and carbon allocation to the tree stem in the  
1340 boreal forest. *Biogeosciences* 14, 4851.

1341 Gessler, A., Ferrio, J.P., Hommel, R., Treydte, K., Werner, R.A., Monson, R.K., 2014. Stable  
1342 isotopes in tree rings: towards a mechanistic understanding of isotope fractionation and  
1343 mixing processes from the leaves to the wood. *Tree physiology* 34, 796-818.

1344 Girardin, M.P., Bouriaud, O., Hogg, E.H., Kurz, W., Zimmermann, N.E., Metsaranta, J.M.,  
1345 de Jong, R., Frank, D.C., Esper, J., Büntgen, U., Guo, X.J., Bhatti, J., 2016. No growth  
1346 stimulation of Canada's boreal forest under half-century of combined warming and CO<sub>2</sub>  
1347 fertilization. *Proceedings of the National Academy of Sciences*.

1348 Girardin, M.P., Guo, X.J., De Jong, R., Kinnard, C., Bernier, P., Raulier, F., 2014. Unusual  
1349 forest growth decline in boreal North America covaries with the retreat of Arctic sea ice.  
1350 *Global change biology* 20, 851-866.

1351 Griebel, A., Bennett, L.T., Arndt, S.K., 2017. Evergreen and ever growing—Stem and canopy  
1352 growth dynamics of a temperate eucalypt forest. *Forest Ecology and Management* 389,  
1353 417-426.

1354 Grossiord, C., Granier, A., Ratcliffe, S., Bouriaud, O., Bruelheide, H., Chećko, E., Forrester,  
1355 D.I., Dawud, S.M., Finér, L., Pollastrini, M., 2014. Tree diversity does not always  
1356 improve resistance of forest ecosystems to drought. *Proceedings of the National Academy*  
1357 *of Sciences* 111, 14812-14815.

1358 Guiot, J., Boucher, E., Gea-Izquierdo, G., 2014. Process models and model-data fusion in  
1359 dendroecology. *Frontiers in Ecology and Evolution* 2, 52.

1360 Gustafson, E.J., 2013. When relationships estimated in the past cannot be used to predict the  
1361 future: using mechanistic models to predict landscape ecological dynamics in a changing  
1362 world. *Landscape ecology* 28, 1429-1437.

1363 Harris, I., Jones, P., Osborn, T., Lister, D., 2014. Updated high - resolution grids of monthly  
1364 climatic observations-the CRU TS3. 10 Dataset. *International Journal of Climatology* 34,  
1365 623-642.

1366 Hayat, A., Hackett-Pain, A.J., Pretzsch, H., Rademacher, T.T., Friend, A.D., 2017. Modeling  
1367 Tree Growth Taking into Account Carbon Source and Sink Limitations. *Frontiers in plant*  
1368 *science* 8.

1369 Hellmann, L., Agafonov, L., Ljungqvist, F.C., Churakova, O., Dũthorn, E., Esper, J.,  
1370 Hũlsmann, L., Kirďyanov, A.V., Moiseev, P., Myglan, V.S., 2016. Diverse growth trends  
1371 and climate responses across Eurasia’s boreal forest. *Environmental Research Letters* 11,  
1372 074021.

1373 Hũlttũ, T., Mũkinen, H., Nũjd, P., Mũkelũ, A., Nikinmaa, E., 2010. A physiological model of  
1374 softwood cambial growth. *Tree Physiology* 30, 1235-1252.

1375 Housset, J.M., Nadeau, S., Isabel, N., Depardieu, C., Duchesne, I., Lenz, P., Girardin, M.P.,  
1376 2018. Tree rings provide a new class of phenotypes for genetic associations that foster  
1377 insights into adaptation of conifers to climate change. *New Phytologist*.

1378 Howard, R., Wilson, B., 1972. A stochastic model for cambial activity. *Botanical Gazette*  
1379 133, 410-414.

1380 Huang, K., Yi, C., Wu, D., Zhou, T., Zhao, X., Blanford, W.J., Wei, S., Wu, H., Ling, D., Li,  
1381 Z., 2015. Tipping point of a conifer forest ecosystem under severe drought. *Environmental*  
1382 *Research Letters* 10, 024011.

1383 Jucker, T., Caspersen, J., Chave, J., Antin, C., Barbier, N., Bongers, F., Dalponte, M., Ewijk,  
1384 K.Y., Forrester, D.I., Haeni, M., 2017. Allometric equations for integrating remote sensing  
1385 imagery into forest monitoring programmes. *Global change biology* 23, 177-190.

1386 Kaufmann, R., D’arrigo, R., Laskowski, C., Myneni, R., Zhou, L., Davi, N., 2004. The effect  
1387 of growing season and summer greenness on northern forests. *Geophysical research letters*  
1388 31.

1389 Klesse, S., Etzold, S., Frank, D., 2016. Integrating tree-ring and inventory-based  
1390 measurements of aboveground biomass growth: research opportunities and carbon cycle  
1391 consequences from a large snow breakage event in the Swiss Alps. *European journal of*  
1392 *forest research* 135, 297-311.

1393 Kũrner, C., 2015. Paradigm shift in plant growth control. *Current Opinion in Plant Biology*  
1394 25, 107-114.

1395 Kũrner, C., 2017. A matter of tree longevity. *Science* 355, 130-131.

1396 Le Quũrũ, C., Andrew, R.M., Canadell, J.G., Sitch, S., Korsbakken, J.I., Peters, G.P.,  
1397 Manning, A.C., Boden, T.A., Tans, P.P., Houghton, R.A., 2016. Global carbon budget  
1398 2016. *Earth System Science Data* 8, 605-649.

- 1399 Levesque, M., Andreu-Hayles, L., Pederson, N., 2017. Water availability drives gas exchange  
1400 and growth of trees in northeastern US, not elevated CO<sub>2</sub> and reduced acid deposition.  
1401 *Scientific Reports* 7.
- 1402 Li, G., Harrison, S., Prentice, I., Falster, D., 2014. Simulation of tree-ring widths with a  
1403 model for primary production, carbon allocation, and growth.
- 1404 Liski, J., Kaasalainen, S., Raunonen, P., Akujärvi, A., Krooks, A., Repo, A., Kaasalainen,  
1405 M., 2014. Indirect emissions of forest bioenergy: detailed modeling of stump - root  
1406 systems. *Gcb Bioenergy* 6, 777-784.
- 1407 Madrigal-González, J., Ballesteros-Cánovas, J.A., Herrero, A., Ruiz-Benito, P., Stoffel, M.,  
1408 Lucas-Borja, M.E., Andivia, E., Sancho-García, C., Zavala, M.A., 2017. Forest  
1409 productivity in southwestern Europe is controlled by coupled North Atlantic and Atlantic  
1410 Multidecadal Oscillations. *Nature communications* 8, 2222.
- 1411 Marotzke, J., Jakob, C., Bony, S., Dirmeyer, P.A., O’Gorman, P.A., Hawkins, E., Perkins-  
1412 Kirkpatrick, S., Le Quéré, C., Nowicki, S., Paulavets, K., 2017. Climate research must  
1413 sharpen its view. *Nature Climate Change* 7, 89.
- 1414 Martin - Benito, D., Pederson, N., 2015. Convergence in drought stress, but a divergence of  
1415 climatic drivers across a latitudinal gradient in a temperate broadleaf forest. *Journal of*  
1416 *Biogeography* 42, 925-937.
- 1417 McRoberts, R.E., Tomppo, E., Schadauer, K., Vidal, C., Ståhl, G., Chirici, G., Lanz, A.,  
1418 Cienciala, E., Winter, S., Smith, W.B., 2009. Harmonizing national forest inventories.  
1419 *Journal of Forestry* 107, 179-187.
- 1420 Melvin, T.M., Briffa, K.R., 2008. A “signal-free” approach to dendroclimatic standardisation.  
1421 *Dendrochronologia* 26, 71-86.
- 1422 Mendivelso, H.A., Camarero, J.J., Gutiérrez, E., Zuidema, P.A., 2014. Time-dependent  
1423 effects of climate and drought on tree growth in a Neotropical dry forest: Short-term  
1424 tolerance vs. long-term sensitivity. *Agricultural and Forest Meteorology* 188, 13-23.
- 1425 Mina, M., Martin-Benito, D., Bugmann, H., Cailleret, M., 2016. Forward modeling of tree-  
1426 ring width improves simulation of forest growth responses to drought. *Agricultural and*  
1427 *Forest Meteorology* 221, 13-33.
- 1428 Misson, L., 2004. MAIDEN: a model for analyzing ecosystem processes in dendroecology.  
1429 *Canadian Journal of Forest Research* 34, 874-887.
- 1430 Monserud, R.A., Marshall, J.D., 2001. Time-series analysis of  $\delta^{13}\text{C}$  from tree rings. I. Time  
1431 trends and autocorrelation. *Tree physiology* 21, 1087-1102.
- 1432 Montané, F., Fox, A.M., Arellano, A.F., MacBean, N., Alexander, M.R., Dye, A., Bishop,  
1433 D.A., Trouet, V., Babst, F., Hessler, A.E., 2017. Evaluating the effect of alternative carbon  
1434 allocation schemes in a land surface model (CLM4. 5) on carbon fluxes, pools, and  
1435 turnover in temperate forests. *Geoscientific Model Development* 10, 3499.
- 1436 Morales, M., Carilla, J., Grau, H., Villalba, R., 2015. Multi-century lake area changes in the  
1437 Southern Altiplano: a tree-ring-based reconstruction. *Climate of the Past* 11, 1139.
- 1438 Nash, J.E., Sutcliffe, J.V., 1970. River flow forecasting through conceptual models part I—A  
1439 discussion of principles. *Journal of hydrology* 10, 282-290.
- 1440 Nehrbass - Ahles, C., Babst, F., Klesse, S., Nötzli, M., Bouriaud, O., Neukom, R., Dobbertin,  
1441 M., Frank, D., 2014. The influence of sampling design on tree - ring - based  
1442 quantification of forest growth. *Global change biology* 20, 2867-2885.
- 1443 Neukom, R., Gergis, J., Karoly, D.J., Wanner, H., Curran, M., Elbert, J., González-Rouco, F.,  
1444 Linsley, B.K., Moy, A.D., Mundo, I., 2014. Inter-hemispheric temperature variability over  
1445 the past millennium. *Nature Climate Change* 4, 362.
- 1446 Newnham, G.J., Armston, J.D., Calders, K., Disney, M.I., Lovell, J.L., Schaaf, C.B., Strahler,  
1447 A.H., Danson, F.M., 2015. Terrestrial laser scanning for plot-scale forest measurement.  
1448 *Current Forestry Reports* 1, 239-251.



- 1449 Nicklen, E.F., Roland, C.A., Ruess, R.W., Schmidt, J.H., Lloyd, A.H., 2016. Local site  
1450 conditions drive climate–growth responses of *Picea mariana* and *Picea glauca* in interior  
1451 Alaska. *Ecosphere* 7.
- 1452 Nickless, A., Scholes, R.J., Archibald, S., 2011. A method for calculating the variance and  
1453 confidence intervals for tree biomass estimates obtained from allometric equations. *South  
1454 African Journal of Science* 107, 1-10.
- 1455 Ogle, K., Barber, J.J., Barron - Gafford, G.A., Bentley, L.P., Young, J.M., Huxman, T.E.,  
1456 Loik, M.E., Tissue, D.T., 2015. Quantifying ecological memory in plant and ecosystem  
1457 processes. *Ecology letters* 18, 221-235.
- 1458 Ols, C., Girardin, M.P., Hofgaard, A., Bergeron, Y., Drobyshev, I., 2017. Monitoring climate  
1459 sensitivity shifts in tree-rings of eastern boreal North America using model-data  
1460 comparison. *Ecosystems*, 1-16.
- 1461 Omernik, J.M., Griffith, G.E., 2014. Ecoregions of the conterminous United States: evolution  
1462 of a hierarchical spatial framework. *Environmental management* 54, 1249-1266.
- 1463 Pappas, C., Mahecha, M.D., Frank, D.C., Babst, F., Koutsoyiannis, D., 2017. Ecosystem  
1464 functioning is enveloped by hydrometeorological variability. *Nature ecology & evolution*  
1465 1, 1263.
- 1466 Pasho, E., Alla, A.Q., 2015. Climate impacts on radial growth and vegetation activity of two  
1467 co-existing Mediterranean pine species. *Canadian Journal of Forest Research* 45, 1748-  
1468 1756.
- 1469 Peng, C., Guiot, J., Wu, H., Jiang, H., Luo, Y., 2011. Integrating models with data in ecology  
1470 and palaeoecology: advances towards a model–data fusion approach. *Ecology Letters* 14,  
1471 522-536.
- 1472 Peñuelas, J., Canadell, J.G., Ogaya, R., 2011. Increased water - use efficiency during the  
1473 20th century did not translate into enhanced tree growth. *Global Ecology and  
1474 Biogeography* 20, 597-608.
- 1475 Peters, K., Jacoby, G.C., Cook, E.R., 1981. Principal components analysis of tree-ring sites.
- 1476 Peters, R.L., Groenendijk, P., Vlam, M., Zuidema, P.A., 2015. Detecting long - term growth  
1477 trends using tree rings: a critical evaluation of methods. *Global change biology* 21, 2040-  
1478 2054.
- 1479 Poulter, B., Pederson, N., Liu, H., Zhu, Z., D'Arrigo, R., Ciais, P., Davi, N., Frank, D.,  
1480 Leland, C., Myneni, R., Piao, S., Wang, T., 2013. Recent trends in Inner Asian forest  
1481 dynamics to temperature and precipitation indicate high sensitivity to climate change.  
1482 *Agricultural and Forest Meteorology* 178-179, 31-45.
- 1483 Rathgeber, C.B., Cuny, H.E., Fonti, P., 2016. Biological basis of tree-ring formation: a crash  
1484 course. *Frontiers in plant science* 7.
- 1485 Restaino, C.M., Peterson, D.L., Littell, J., 2016. Increased water deficit decreases Douglas fir  
1486 growth throughout western US forests. *Proceedings of the National Academy of Sciences*  
1487 113, 9557-9562.
- 1488 Richardson, A.D., Carbone, M.S., Keenan, T.F., Czimczik, C.I., Hollinger, D.Y., Murakami,  
1489 P., Schaberg, P.G., Xu, X., 2013. Seasonal dynamics and age of stemwood nonstructural  
1490 carbohydrates in temperate forest trees. *New Phytologist* 197, 850-861.
- 1491 Rollinson, C.R., Kaye, M.W., Canham, C.D., 2016. Interspecific variation in growth  
1492 responses to climate and competition of five eastern tree species. *Ecology* 97, 1003-1011.
- 1493 Rollinson, C.R., Liu, Y., Raiho, A., Moore, D.J., McLachlan, J., Bishop, D.A., Dye, A.,  
1494 Matthes, J.H., Hessler, A., Hickler, T., 2017. Emergent climate and CO2 sensitivities of net  
1495 primary productivity in ecosystem models do not agree with empirical data in temperate  
1496 forests of eastern North America. *Global change biology*.

- 1497 Rossi, S., Anfodillo, T., Čufar, K., Cuny, H.E., Deslauriers, A., Fonti, P., Frank, D., Gričar,  
1498 J., Gruber, A., Huang, J.G., 2016. Pattern of xylem phenology in conifers of cold  
1499 ecosystems at the Northern Hemisphere. *Global change biology* 22, 3804-3813.
- 1500 Salzer, M.W., Hughes, M.K., Bunn, A.G., Kipfmüller, K.F., 2009. Recent unprecedented  
1501 tree-ring growth in bristlecone pine at the highest elevations and possible causes.  
1502 *Proceedings of the National Academy of Sciences* 106, 20348-20353.
- 1503 Salzer, M.W., Larson, E.R., Bunn, A.G., Hughes, M.K., 2014. Changing climate response in  
1504 near-treeline bristlecone pine with elevation and aspect. *Environmental Research Letters*  
1505 9, 114007.
- 1506 Sánchez-Salguero, R., Linares, J.C., Camarero, J.J., Madrigal-González, J., Hevia, A.,  
1507 Sánchez-Miranda, Á., Ballesteros-Cánovas, J.A., Alfaro-Sánchez, R., García-Cervigón,  
1508 A.I., Bigler, C., 2015. Disentangling the effects of competition and climate on individual  
1509 tree growth: a retrospective and dynamic approach in Scots pine. *Forest Ecology and*  
1510 *Management* 358, 12-25.
- 1511 Sangüesa-Barreda, G., Camarero, J.J., García-Martín, A., Hernández, R., de la Riva, J., 2014.  
1512 Remote-sensing and tree-ring based characterization of forest defoliation and growth loss  
1513 due to the Mediterranean pine processionary moth. *Forest Ecology and Management* 320,  
1514 171-181.
- 1515 Scholes, R.J., 2017. Taking the mumbo out of the jumbo: progress towards a robust basis for  
1516 ecological scaling. *Ecosystems* 20, 4-13.
- 1517 Schwalm, C.R., Anderegg, W.R., Michalak, A.M., Fisher, J.B., Biondi, F., Koch, G., Litvak,  
1518 M., Ogle, K., Shaw, J.D., Wolf, A., 2017. Global patterns of drought recovery. *Nature*  
1519 548, 202.
- 1520 Schwalm, C.R., Williams, C.A., Schaefer, K., Baldocchi, D., Black, T.A., Goldstein, A.H.,  
1521 Law, B.E., Oechel, W.C., Scott, R.L., 2012. Reduction in carbon uptake during turn of the  
1522 century drought in western North America. *Nature Geoscience* 5, 551-556.
- 1523 Seftigen, K., Frank, D.C., Björklund, J., Babst, F., Poulter, B., in press, The climatic drivers  
1524 of NDVI and tree-ring based estimates of forest productivity are spatially coherent but  
1525 temporally decoupled in Northern Hemispheric forests. *Global Ecology and*  
1526 *Biogeography*.
- 1527 Seim, A., Treydte, K., Trouet, V., Frank, D., Fonti, P., Tegel, W., Panayotov, M.,  
1528 Fernández - Donado, L., Krusic, P., Büntgen, U., 2015. Climate sensitivity of  
1529 Mediterranean pine growth reveals distinct east-west dipole. *International journal of*  
1530 *climatology* 35, 2503-2513.
- 1531 Serra-Diaz, J.M., Enquist, B.J., Maitner, B., Merow, C., Svenning, J.-C., 2017. Big data of  
1532 tree species distributions: how big and how good? *Forest Ecosystems* 4, 30.
- 1533 Shi, J., Liu, Y., Vaganov, E.A., Li, J., Cai, Q., 2008. Statistical and process - based modeling  
1534 analyses of tree growth response to climate in semi - arid area of north central China: A  
1535 case study of *Pinus tabulaeformis*. *Journal of Geophysical Research: Biogeosciences* 113.
- 1536 Shishov, V.V., Tychkov, I.I., Popkova, M.I., Ilyin, V.A., Bryukhanova, M.V., Kirilyanov,  
1537 A.V., 2016. VS-oscilloscope: A new tool to parameterize tree radial growth based on  
1538 climate conditions. *Dendrochronologia* 39, 42-50.
- 1539 Sitch, S., Friedlingstein, P., Gruber, N., Jones, S., Murray-Tortarolo, G., Ahlström, A.,  
1540 Doney, S.C., Graven, H., Heinze, C., Huntingford, C., 2015. Recent trends and drivers of  
1541 regional sources and sinks of carbon dioxide. *Biogeosciences* 12, 653-679.
- 1542 St George, S., Ault, T.R., 2014. The imprint of climate within Northern Hemisphere trees.  
1543 *Quaternary Science Reviews* 89, 1-4.
- 1544 Stevens, D.W., 1975. A computer program for simulating cambial activity and ring growth.  
1545 *Tree-Ring Bulletin*.

- 1546 Stokes, M.A., Smiley, T.L., 1968. An introduction to tree-ring dating. University of Chicago,  
1547 Chicago, Reprinted 1996. University of Arizona Press, Tucson.
- 1548 Sullivan, P.F., Csank, A.Z., 2016. Contrasting sampling designs among archived datasets:  
1549 implications for synthesis efforts. *Tree physiology* 36, 1057-1059.
- 1550 Swetnam, T.W., Allen, C.D., Betancourt, J.L., 1999. Applied historical ecology: using the  
1551 past to manage for the future. *Ecological applications* 9, 1189-1206.
- 1552 Tang, L., Shao, G., 2015. Drone remote sensing for forestry research and practices. *Journal of*  
1553 *Forestry Research* 26, 791-797.
- 1554 Teets, A., Fraver, S., Weiskittel, A.R., Hollinger, D.Y., 2018. Quantifying climate-growth  
1555 relationships at the stand level in a mature mixed - species conifer forest. *Global change*  
1556 *biology*.
- 1557 Tei, S., Sugimoto, A., Yonenobu, H., Matsuura, Y., Osawa, A., Sato, H., Fujinuma, J.,  
1558 Maximov, T., 2017. Tree - ring analysis and modeling approaches yield contrary response  
1559 of circumboreal forest productivity to climate change. *Global Change Biology*.
- 1560 Tolwinski-Ward, S., Evans, M.N., Hughes, M.K., Anchukaitis, K.J., 2011. An efficient  
1561 forward model of the climate controls on interannual variation in tree-ring width. *Climate*  
1562 *Dynamics* 36, 2419-2439.
- 1563 Touchan, R., Shishov, V., Meko, D., Nouri, I., Grachev, A., 2012. Process based model  
1564 sheds light on climate sensitivity of Mediterranean tree-ring width. *Biogeosciences* 9, 965.
- 1565 Trotsiuk, V., Svoboda, M., Weber, P., Pederson, N., Klesse, S., Janda, P., Martin-Benito, D.,  
1566 Mikolas, M., Seedre, M., Bace, R., 2016. The legacy of disturbance on individual tree and  
1567 stand-level aboveground biomass accumulation and stocks in primary mountain *Picea*  
1568 *abies* forests. *Forest Ecology and Management* 373, 108-115.
- 1569 Trouet, V., Babst, F., Meko, M., 2018. Recent enhanced high-summer North Atlantic Jet  
1570 variability emerges from three-century context. *Nature Communications* 9, 180.
- 1571 Trouet, V., Mukelabai, M., Verheyden, A., Beeckman, H., 2012. Cambial growth season of  
1572 brevi-deciduous *Brachystegia spiciformis* trees from South Central Africa restricted to less  
1573 than four months. *PLoS One* 7, e47364.
- 1574 Tucker, C.J., Pinzon, J.E., Brown, M.E., Slayback, D.A., Pak, E.W., Mahoney, R., Vermote,  
1575 E.F., El Saleous, N., 2005. An extended AVHRR 8 - km NDVI dataset compatible with  
1576 MODIS and SPOT vegetation NDVI data. *International Journal of Remote Sensing* 26,  
1577 4485-4498.
- 1578 Vaganov, E.A., Hughes, M.K., Shashkin, A.V., 2006. *Growth Dynamics of Conifer Tree*  
1579 *Rings: Images of Past and Future Environments* Springer, New York.
- 1580 van der Maaten-Theunissen, M., Bouriaud, O., 2012. Climate-growth relationships at  
1581 different stem heights in silver fir and Norway spruce. *Canadian Journal of Forest*  
1582 *Research* 42, 958-969.
- 1583 Vicente-Serrano, S.M., Camarero, J.J., Olano, J.M., Martín-Hernández, N., Peña-Gallardo,  
1584 M., Tomás-Burguera, M., Gazol, A., Azorin-Molina, C., Bhuyan, U., El Kenawy, A.,  
1585 2016. Diverse relationships between forest growth and the Normalized Difference  
1586 Vegetation Index at a global scale. *Remote Sensing of Environment* 187, 14-29.
- 1587 Vicente-Serrano, S.M., Gouveia, C., Camarero, J.J., Beguería, S., Trigo, R., López-Moreno,  
1588 J.I., Azorín-Molina, C., Pasho, E., Lorenzo-Lacruz, J., Revuelto, J., 2013. Response of  
1589 vegetation to drought time-scales across global land biomes. *Proceedings of the National*  
1590 *Academy of Sciences* 110, 52-57.
- 1591 von Arx, G., Crivellaro, A., Prendin, A.L., Čufar, K., Carrer, M., 2016. Quantitative wood  
1592 anatomy—practical guidelines. *Frontiers in plant science* 7.
- 1593 Wagner, B., Ginzler, C., Bürgi, A., Santini, S., Gärtner, H., 2017. An annually-resolved stem  
1594 growth tool based on 3D laser scans and 2D tree-ring data. *Trees*, 1-12.

1595 Westoby, M., Brasington, J., Glasser, N., Hambrey, M., Reynolds, J., 2012. 'Structure-from-  
1596 Motion' photogrammetry: A low-cost, effective tool for geoscience applications.  
1597 *Geomorphology* 179, 300-314.

1598 Wigley, T.M.L., Briffa, K.R., Jones, P.D., 1984. ON THE AVERAGE VALUE OF  
1599 CORRELATED TIME-SERIES, WITH APPLICATIONS IN  
1600 DENDROCLIMATOLOGY AND HYDROMETEOROLOGY. *Journal of Climate and  
1601 Applied Meteorology* 23, 201-213.

1602 Wilkinson, S., Ogée, J., Domec, J.-C., Rayment, M., Wingate, L., 2015. Biophysical  
1603 modelling of intra-ring variations in tracheid features and wood density of *Pinus pinaster*  
1604 trees exposed to seasonal droughts. *Tree physiology* 35, 305-318.

1605 Williams, A.P., Allen, C.D., Macalady, A.K., Griffin, D., Woodhouse, C.A., Meko, D.M.,  
1606 Swetnam, T.W., Rauscher, S.A., Seager, R., Grissino-Mayer, H.D., 2013. Temperature as  
1607 a potent driver of regional forest drought stress and tree mortality. *Nature Climate Change*  
1608 3, 292-297.

1609 Wilson, B., 1973. A diffusion model for tracheid production and enlargement in conifers.  
1610 *Botanical Gazette* 134, 189-196.

1611 Wilson, B.F., Howard, R.A., 1968. A computer model for cambial activity. *Forest Science*  
1612 14, 77-90.

1613 Wilson, R., Anchukaitis, K., Briffa, K.R., Büntgen, U., Cook, E., D'arrigo, R., Davi, N.,  
1614 Esper, J., Frank, D., Gunnarson, B., 2016. Last millennium northern hemisphere summer  
1615 temperatures from tree rings: Part I: The long term context. *Quaternary Science Reviews*  
1616 134, 1-18.

1617 Wu, X., Liu, H., Li, X., Ciais, P., Babst, F., Guo, W., Zhang, C., Magliulo, V., Pavelka, M.,  
1618 Liu, S., 2017. Differentiating drought legacy effects on vegetation growth over the  
1619 temperate Northern Hemisphere. *Global change biology*.

1620 Zhang, Y., Shao, X., Xu, Y., Wilmking, M., 2011. Process-based modeling analyses of  
1621 *Sabina przewalskii* growth response to climate factors around the northeastern Qaidam  
1622 Basin. *Chinese Science Bulletin* 56, 1518-1525.

1623 Zhang, Z., Babst, F., Bellassen, V., Frank, D., Launois, T., Tan, K., Ciais, P., Poulter, B.,  
1624 Converging Climate Sensitivities of European Forests Between Observed Radial Tree  
1625 Growth and Vegetation Models. *Ecosystems*, 1-16.

1626 Zhang, Z., Babst, F., Bellassen, V., Frank, D., Launois, T., Tan, K., Ciais, P., Poulter, B.,  
1627 2017. Converging Climate Sensitivities of European Forests Between Observed Radial  
1628 Tree Growth and Vegetation Models. *Ecosystems*.

1629 Zhang, Z., Babst, F., Bellassen, V., Frank, D., Launois, T., Tan, K., Ciais, P., Poulter, B.,  
1630 2018. Converging climate sensitivities of European forests between observed radial tree  
1631 growth and vegetation models. *Ecosystems* 21, 410-425.

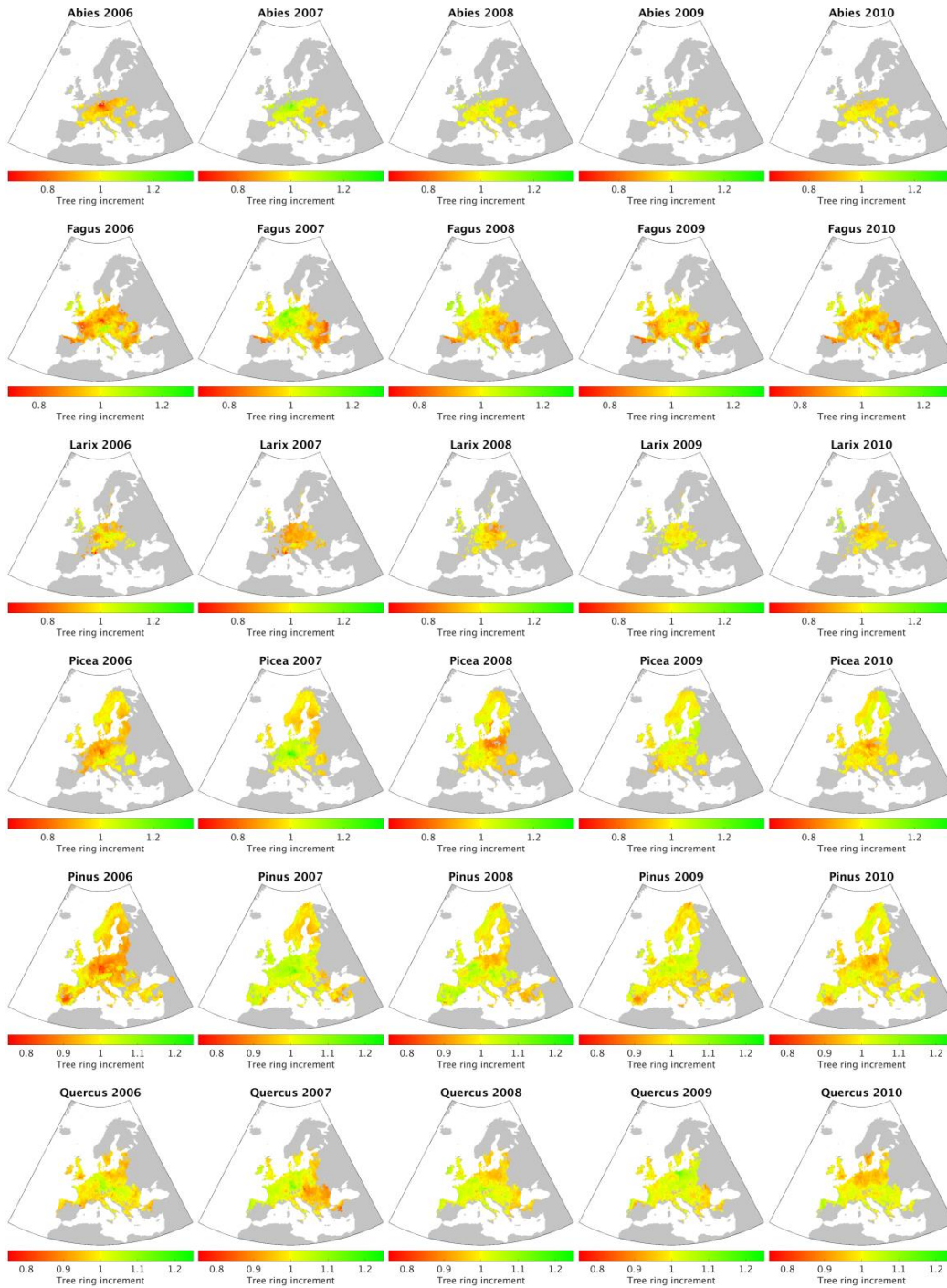
1632 Zhu, Z., Piao, S., Myneni, R.B., Huang, M., Zeng, Z., Canadell, J.G., Ciais, P., Sitch, S.,  
1633 Friedlingstein, P., Arneeth, A., 2016. Greening of the Earth and its drivers. *Nature climate  
1634 change* 6, 791-795.

1635 Zuidema, P.A., Frank, D., 2015. Forests: Tree rings track climate trade-offs. *Nature* 523, 531.  
1636

1637 **Appendix A: Supplementary figure**

1638

1639



1640

1641

1642

1643

1644

1645

**Figure S1:** Gridded tree-ring width anomalies (increment) between 2006-2010 for the six tree genera that occur most frequently in the International Tree Ring Data Bank. The maps were produced using the random decision forest approach presented in Figure 2 of the main manuscript.